

---



---

# Report of the Quark Flavor Physics Working Group

Conveners: J.N. Butler,<sup>13</sup> Z. Ligeti,<sup>22</sup> J.L. Ritchie<sup>38</sup>

Task Force leaders:

V. Cirigliano,<sup>23</sup> S. Kettell<sup>3</sup> (Kaons); R. Briere,<sup>6</sup> A.A. Petrov<sup>13</sup> (Charm);  
A. Schwartz,<sup>8</sup> T. Skwarnicki,<sup>37</sup> J. Zupan<sup>8</sup> (*B* physics);  
N. Christ,<sup>10</sup> S.R. Sharpe,<sup>41</sup> R.S. Van de Water<sup>13</sup> (Lattice QCD)

W. Altmannshofer,<sup>13</sup> N. Arkani-Hamed,<sup>20</sup> M. Artuso,<sup>37</sup> D.M. Asner,<sup>32</sup> C. Bernard,<sup>42</sup> A.J. Bevan,<sup>34</sup>  
M. Blanke,<sup>12</sup> G. Bonvicini,<sup>13</sup> T.E. Browder,<sup>17</sup> D.A. Bryman,<sup>2</sup> P. Campana,<sup>14</sup> R. Cenci,<sup>24</sup> D. Cline,<sup>4</sup>  
J. Comfort,<sup>1</sup> D. Cronin-Hennessy,<sup>26</sup> A. Datta,<sup>27</sup> S. Dobbs,<sup>29</sup> M. Duraisamy,<sup>27</sup> A.X. El-Khadra,<sup>18</sup>  
J.E. Fast,<sup>32</sup> R. Forty,<sup>12</sup> K.T. Flood,<sup>5</sup> T. Gershon,<sup>40</sup> Y. Grossman,<sup>11</sup> B. Hamilton,<sup>24</sup> C.T. Hill,<sup>13</sup>  
R.J. Hill,<sup>7</sup> D.G. Hitlin,<sup>5</sup> D.E. Jaffe,<sup>3</sup> A. Jawahery,<sup>24</sup> C.P. Jessop,<sup>28</sup> A.L. Kagan,<sup>8</sup> D.M. Kaplan,<sup>19</sup>  
M. Kohl,<sup>16</sup> P. Krizan,<sup>21</sup> A.S. Kronfeld,<sup>13</sup> K. Lee,<sup>4</sup> L.S. Littenberg,<sup>3</sup> D.B. MacFarlane,<sup>35</sup> P.B. Mackenzie,<sup>13</sup>  
B.T. Meadows,<sup>8</sup> J. Olsen,<sup>33</sup> M. Papucci,<sup>22</sup> Z. Parsa,<sup>3</sup> G. Paz,<sup>13</sup> G. Perez,<sup>12,44</sup> L.E. Piilonen,<sup>39</sup> K. Pitts,<sup>18</sup>  
M.V. Purohit,<sup>36</sup> B. Quinn,<sup>27</sup> B.N. Ratcliff,<sup>35</sup> D.A. Roberts,<sup>24</sup> J.L. Rosner,<sup>7</sup> P. Rubin,<sup>15</sup> J. Seeman,<sup>35</sup>  
K.K. Seth,<sup>29</sup> B. Schmidt,<sup>12</sup> A. Schopper,<sup>12</sup> M.D. Sokoloff,<sup>8</sup> A. Soni,<sup>3</sup> K. Stenson,<sup>9</sup> S. Stone,<sup>37</sup>  
R. Sundrum,<sup>24</sup> R. Tschirhart,<sup>13</sup> A. Vainshtein,<sup>26</sup> Y.W. Wah,<sup>7</sup> G. Wilkinson,<sup>31</sup> M.B. Wise,<sup>5</sup>  
E. Worcester,<sup>3</sup> J. Xu,<sup>25</sup> T. Yamanaka<sup>30</sup>

<sup>1</sup>Arizona State University, Tempe, AZ 85287-1504, USA

<sup>2</sup>University of British Columbia, Vancouver, BC V1V 1V7, Canada

<sup>3</sup>Brookhaven National Laboratory, Upton, NY 11973-5000, USA

<sup>4</sup>University of California, Los Angeles, Los Angeles, CA 90095, USA

<sup>5</sup>California Institute of Technology, Pasadena, CA 91125, USA

<sup>6</sup>Carnegie Mellon University, Pittsburgh, PA 15213, USA

<sup>7</sup>University of Chicago, Enrico Fermi Institute, Chicago, IL 60637, USA

<sup>8</sup>University of Cincinnati, Cincinnati, OH 45221, USA

<sup>9</sup>University of Colorado, Boulder, CO 80309, USA

<sup>10</sup>Columbia University, New York, NY 10027, USA

<sup>11</sup>Cornell University, Ithaca, NY 14853, USA

<sup>12</sup>European Organization for Nuclear Research (CERN), Geneva, Switzerland

<sup>13</sup>Fermi National Accelerator Laboratory, Batavia, IL 60510, USA

<sup>14</sup>Laboratori Nazionali di Frascati dell'INFN, I-00044 Frascati, Italy

<sup>15</sup>George Mason University, Fairfax, VA 22030, USA

<sup>16</sup>Hampton University, Hampton, VA 23668, USA

<sup>17</sup>University of Hawaii, Honolulu, Hawaii 96822, USA

<sup>18</sup>University of Illinois, Urbana, IL 61801, USA

<sup>19</sup>Illinois Institute of Technology, Chicago, IL 60616, USA

<sup>20</sup>Institute for Advanced Study, Princeton, NJ 08540, USA

<sup>21</sup>Jozef Stefan Institute, 1000 Ljubljana, Slovenia

- <sup>22</sup>Lawrence Berkeley National Laboratory, Berkeley, CA 94720, USA
- <sup>23</sup>Los Alamos National Laboratory, Los Alamos, NM 87545, USA
- <sup>24</sup>University of Maryland, College Park, MD 20742, USA
- <sup>25</sup>University of Michigan, Ann Arbor, MI 48109, USA
- <sup>26</sup>University of Minnesota, Minneapolis, MN 55455 USA
- <sup>27</sup>University of Mississippi, Oxford, MS 38677, USA
- <sup>28</sup>University of Notre Dame, Notre Dame, IN 46556, USA
- <sup>29</sup>Northwestern University, Evanston, IL 60208 USA
- <sup>30</sup>Osaka University, Toyonaka, Osaka 560-0043, Japan
- <sup>31</sup>University of Oxford, Oxford, OX1 3RH, United Kingdom
- <sup>32</sup>Pacific Northwest National Laboratory, Richland, WA 99352
- <sup>33</sup>Princeton University, Princeton, NJ 08544, USA
- <sup>34</sup>Queen Mary University of London, London, E1 4NS, United Kingdom
- <sup>35</sup>SLAC National Accelerator Laboratory, Menlo Park, CA 94025, USA
- <sup>36</sup>University of South Carolina, Columbia, SC 29208, USA
- <sup>37</sup>Syracuse University, Syracuse, NY 13244-5040, USA
- <sup>38</sup>University of Texas at Austin, Austin, TX 78712-0587, USA
- <sup>39</sup>Virginia Polytechnic Institute and State University, Blacksburg, VA 24061, USA
- <sup>40</sup>University of Warwick, Coventry CV4 7AL, United Kingdom
- <sup>41</sup>University of Washington, Seattle, WA 98195 USA
- <sup>42</sup>Washington University, St. Louis, MO 63130, USA
- <sup>43</sup>Wayne State University, Detroit, MI 48201, USA
- <sup>44</sup>Weizmann Institute of Science, Rehovot 76100, Israel

### Abstract

This report represents the response of the Intensity Frontier Quark Flavor Physics Working Group to the Snowmass charge. We summarize the current status of quark flavor physics and identify many exciting future opportunities for studying the properties of strange, charm, and bottom quarks. The ability of these studies to reveal the effects of new physics at high mass scales make them an essential ingredient in a well-balanced experimental particle physics program.

## Table of Contents

1	Introduction . . . . .	4
2	Quark Flavor as a Tool for Discovery . . . . .	5
2.1	Strange, Charm, and Bottom Quarks as Probes for New Physics . . . . .	6
2.2	The Role of Theory . . . . .	8
3	Report of the Kaon Task Force . . . . .	10
3.1	Rare Kaon Decays in the Standard Model: Status and Forecast . . . . .	11
3.2	Beyond the Standard Model Physics Reach . . . . .	11
3.3	Experimental Program . . . . .	14
3.4	Conclusions . . . . .	16
4	Report of the $B$ -Physics Task Force . . . . .	16
4.1	Physics Motivation . . . . .	16
4.2	Physics Potential of $e^+e^-$ Experiments: Belle II . . . . .	18
4.3	Physics Potential of Hadronic Experiments . . . . .	22
5	Report of the Charm Task Force . . . . .	25
5.1	Introduction to Charm Physics . . . . .	25
5.2	Current and Future Experiments . . . . .	26
5.3	Charm Physics Summary and Perspectives Beyond 2020 . . . . .	32
6	Report of the Lattice QCD Task Force . . . . .	32
6.1	Future Lattice Calculations of Kaon Properties . . . . .	35
6.2	Future Lattice Calculations of $D$ -meson Properties . . . . .	36
6.3	Future Lattice Calculations of $B$ -meson Properties . . . . .	37
6.4	Lattice QCD and Flavor Physics: 2018–2030 . . . . .	38
7	A U.S. Plan for Quark Flavor Physics . . . . .	39
7.1	Opportunities in This Decade . . . . .	40
7.2	Opportunities in the Next Decade . . . . .	40
7.3	Conclusions . . . . .	41
	References . . . . .	42

# 1 Introduction

This report, from the Quark Flavor Physics working group, describes the physics case for precision studies of flavor-changing interactions of bottom, charm, and strange quarks, and it discusses the experimental program needed to exploit these physics opportunities. It also discusses the role of theory and the importance of lattice QCD to future progress in this field. The report is the result of a process that began before Snowmass, in the fall of 2011 with the DOE-sponsored workshop on Fundamental Physics at the Intensity Frontier (Rockville, MD). The Heavy Quarks working group from that workshop continued into the Snowmass process, albeit with a change of name to Quark Flavor Physics to better reflect our emphasis on quark flavor mixing. The Heavy Quarks report [1] from that workshop provided a starting point for our Snowmass efforts.

With the initiation of the Snowmass process, our working group grew. Also, four Task Forces were organized to focus on four closely related, but distinct, areas of effort in quark-flavor physics: kaons, charm,  $B$ -physics, and lattice QCD. Our working group had physical meetings during the Community Planning Meeting at Fermilab (October, 2012), at the Intensity Frontier Workshop at Argonne (April, 2013), and at Snowmass itself at the University of Minnesota (July, 2013). Consequently, this report is the culmination of discussions that were conducted over a period of almost two years.

This report describes the physics case for quark-flavor physics, and it represents the aspirations of a substantial community of physicists in the U.S. who are interested in this physics. This report is not a review of quark-flavor physics, and no attempt has been made to provide complete references to prior work. Rather, it focuses on the opportunities for spectacular discoveries during the remainder of this decade and during the next decade, made possible by the extraordinary reach to high mass scales that is possible in quark-flavor physics experiments.

Nevertheless, before looking forward, it provides useful context to briefly review some history. In the 1990's, the U.S. was the leader both on the Energy Frontier and in quark flavor-physics experiments at the Intensity Frontier.  $B$  physics was still dominated by the CLEO experiment for most of that decade. The most sensitive rare  $K$  decay experiments performed to date were then underway at the Brookhaven AGS, including an experiment that made the first observation of the extremely rare  $K^+ \rightarrow \pi^+ \nu \bar{\nu}$  decay, and a fixed-target experiment using the Tevatron at Fermilab was underway that observed direct CP violation in  $K_L^0 \rightarrow \pi\pi$  decays. Toward the end of that decade, the asymmetric  $e^+e^-$   $B$  factories began running at SLAC and KEK, leading to increases in the size of  $B$  meson data sets by two orders of magnitude and also opening the door to measurements of time-dependent CP asymmetries, which provided the experimental basis for the 2008 Nobel Prize. In the midst of this success, a number of new and ambitious quark-flavor initiatives were put forward in the U.S. These included the BTeV proposal which would have used the Tevatron collider for  $B$  physics, the CKM proposal which would have made the first high-statistics measurement of  $K^+ \rightarrow \pi^+ \nu \bar{\nu}$  using the Fermilab Main Injector, and the RSVP proposal which included an experiment (KOPIO) to measure  $K_L^0 \rightarrow \pi^0 \nu \bar{\nu}$  at the Brookhaven AGS. After lengthy consideration in an environment characterized by flat budgets and a predilection for a fast start on the International Linear Collider on U.S. soil, all of these initiatives were ultimately terminated. Also, as accelerator breakthroughs capable of increasing  $B$ -factory luminosity by more than another order of magnitude were made, the opportunity to upgrade the PEP-II  $B$  factory at SLAC was not pursued. This history is relevant in order to stress that the U.S. has been a leader in flavor-physics experiments — involving a vigorous community — until very recently. Nonetheless, this sequence of events inevitably encouraged many in the flavor-physics community in the U.S. to migrate elsewhere, most often to ATLAS or CMS at the LHC.

In spite of these developments in the U.S., strong physics imperatives have motivated a rich quark flavor physics program that is flourishing around the world. Kaon experiments,  $B$ -physics experiments, and charm experiments are running and under construction in Asia and Europe. Indeed, CERN — the laboratory that

now owns the Energy Frontier — is also the home of a running  $B$ -physics experiment (LHCb), which has a clear upgrade path, and a rare  $K$  decay experiment (NA62), focusing on  $K^+ \rightarrow \pi^+ \nu \bar{\nu}$ , which will begin taking data near the end of 2014. This reflects the world-wide consensus that flavor-physics experiments are critical to progress in particle physics.

Looking forward, it is clear that there continues to be strong interest and a potentially substantial community in the U.S. for an experimental flavor-physics program. The motivation for this program can be described very simply. If the LHC observes new high-mass states, it will be necessary to distinguish among models proposed to explain them. This will require tighter constraints from the flavor sector, which can come from more precise experiments using strange, charm, and bottom quark systems. If the LHC does not make such discoveries, then the ability of precision flavor-physics experiments to probe mass scales far above LHC, through virtual effects, is the best hope to see signals that may point toward the next energy scale to explore.

In the following sections of this report, we describe the general physics case for quark-flavor physics, followed by the reports of each of the Task Forces. The Task Forces were in communication with each other, but worked independently on these reports. Finally, this report concludes with a discussion of how the U.S. high-energy physics program can, at relatively modest cost compared to most other initiatives, participate in critical flavor-physics experiments offshore and regain some of its leadership status by executing a program of rare kaon decay experiments at Fermilab.

## 2 Quark Flavor as a Tool for Discovery

An essential feature of flavor physics experiments is their ability to probe very high mass scales, beyond the energies directly accessible in collider experiments. In addition, flavor physics can teach us about properties of TeV-scale new physics, which cannot be learned from the direct production of new particles at the LHC. This is because quantum effects allow virtual particles to modify the results of precision measurements in ways that reveal the underlying physics. (The determination of the  $t$ - $s$  and  $t$ - $d$  couplings in the standard model (SM) exemplifies how measurements of some properties of heavy particles may only be possible in flavor physics.) Even as the LHC embarks on probing the TeV scale, the ongoing and planned precision flavor physics experiments are sensitive to beyond standard model (BSM) interactions at mass scales which are higher by several orders of magnitude. These experiments will provide essential constraints and complementary information on the structure of models put forth to explain any discoveries at LHC, and they have the potential to reveal new physics that is inaccessible to the LHC.

Throughout the history of particle physics discoveries made in studies of rare processes have led to new and deeper understanding of nature. A classic example is beta decay, which foretold the electroweak mass scale and the ultimate observation of the  $W$  boson. Results from kaon decay experiments were crucial for the development of the standard model: the discovery of CP violation in  $K_L^0 \rightarrow \pi^+ \pi^-$  decay ultimately pointed toward the three-generation CKM model [2, 3], the absence of strangeness-changing neutral current decays (i.e., the suppression of  $K_L^0 \rightarrow \mu^+ \mu^-$  with respect to  $K^+ \rightarrow \mu^+ \nu$ ) led to the prediction of a fourth quark [4] (charm), and the measured value of the  $K_L - K_S$  mass difference made it possible to predict the charm quark mass [5, 6] before charm particles were directly detected. The larger than expected  $B_H - B_L$  mass difference foretold the high mass of the top quark. Precision measurements of time-dependent CP-violating asymmetries in  $B$ -meson decays in the BABAR and Belle experiments firmly established the CKM phase as the dominant source of CP violation observed to date in flavor-changing processes — leading to the 2008 Nobel Prize for Kobayashi and Maskawa. At the same time, corrections to the SM at the tens of percent level are still allowed, and many extensions of the SM proposed to solve the hierarchy problem are likely to give rise to changes in flavor physics that may be observed in the next generation of experiments.

## 2.1 Strange, Charm, and Bottom Quarks as Probes for New Physics

In the past decade our understanding of flavor physics has improved significantly due to the  $e^+e^- B$  factories, BABAR, Belle, CLEO, the Tevatron experiments, and most recently LHCb. While kaon physics was crucial for the development of the SM, and has provided some of the most stringent constraints on BSM physics since the 1960s, precision tests of the CKM picture of CP violation in the kaon sector alone have been hindered by theoretical uncertainties in calculating direct CP violation ( $\epsilon'_K$ ). The  $B$  factories and LHCb provided many stringent tests by precisely measuring numerous CP-violating and CP-conserving quantities, which in the SM are determined in terms of just a few parameters, but are sensitive to different possible BSM contributions. The consistency of the measurements and their agreement with CP violation in  $K^0-\bar{K}^0$  mixing,  $\epsilon_K$ , and with the SM predictions (shown in the left plot in Fig. 1) strengthened the “new physics flavor problem.” It is the tension between the relatively low (TeV) scale required to stabilize the electroweak scale, and the high scale that is seemingly required to suppress BSM contributions to flavor-changing processes. This problem arises because the SM flavor structure is very special, containing small mixing angles, and because of additional strong suppressions of flavor-changing neutral-current (FCNC) processes. Any TeV-scale new physics must preserve these features, which are crucial to explain the observed pattern of weak decays.

The motivation for a broad program of precision flavor physics measurements has gotten even stronger in light of the first LHC run. With the discovery of a new particle whose properties are similar to the SM Higgs boson, but no sign of other high-mass states, the LHC has begun to test naturalness as a guiding principle of BSM research. If the electroweak scale is unnatural, we have little information on the next energy scale to explore (except for a hint at the TeV scale from dark matter, a few anomalous experimental results, and neutrinos most likely pointing at a very high scale). The flavor physics program will explore much higher scales than can be directly probed. However, if the electroweak symmetry breaking scale is stabilized by a natural mechanism, new particles should be found at the LHC. Since the largest quantum correction to the Higgs mass in the SM is due to the top quark, the new particles will likely share some properties of the SM quarks, such as symmetries and interactions. Then they would provide a novel probe of the flavor sector, and flavor physics and the LHC data would provide complementary information. Their combined study is our best chance to learn more about the origin of both electroweak and flavor symmetry breaking.

Consider, for example, a model in which the only suppression of new flavor-changing interactions comes from the large masses of the new particles that mediate them (at a scale  $\Lambda \gg m_W$ ). Flavor physics, in particular measurements of meson mixing and CP violation, put severe lower bounds on  $\Lambda$ . For some of the most important four-quark operators contributing to the mixing of the neutral  $K$ ,  $D$ ,  $B$ , and  $B_s$  mesons, the bounds on the coefficients  $C/\Lambda^2$  are summarized in Table 1. For  $C = 1$ , they are at the scale  $\Lambda \sim (10^2 - 10^5)$  TeV. Conversely, for  $\Lambda = 1$  TeV, the coefficients have to be very small. Therefore, there is a tension. The hierarchy problem can be solved with new physics at  $\Lambda \sim 1$  TeV. Flavor bounds, however, require much larger scales, or tiny couplings. This tension implies that TeV-scale new physics must have special flavor structures, e.g., possibly sharing some of the symmetries that shape the SM Yukawa interactions. The new physics flavor puzzle is thus the question of why, and in what way, the flavor structure of the new physics is non-generic. As a specific example, in a supersymmetric extension of the SM, there are box diagrams with winos and squarks in the loops. The size of such contributions depends crucially on the mechanism of SUSY breaking, which we would like to probe.

To be sensitive to BSM contributions to FCNC processes (where the SM is suppressed, but not absent), many measurements need to be done, and it is only their combination that can reveal a signal. (There are some exceptions, mainly processes forbidden in the SM, but considering only those would reduce the sensitivity of the program to BSM physics.) To visualize the constraints from many measurements, it is convenient to

Operator	Bounds on $\Lambda$ [TeV] ( $C = 1$ )		Bounds on $C$ ( $\Lambda = 1$ TeV)		Observables
	Re	Im	Re	Im	
$(\bar{s}_L \gamma^\mu d_L)^2$	$9.8 \times 10^2$	$1.6 \times 10^4$	$9.0 \times 10^{-7}$	$3.4 \times 10^{-9}$	$\Delta m_K; \epsilon_K$
$(\bar{s}_R d_L)(\bar{s}_L d_R)$	$1.8 \times 10^4$	$3.2 \times 10^5$	$6.9 \times 10^{-9}$	$2.6 \times 10^{-11}$	$\Delta m_K; \epsilon_K$
$(\bar{c}_L \gamma^\mu u_L)^2$	$1.2 \times 10^3$	$2.9 \times 10^3$	$5.6 \times 10^{-7}$	$1.0 \times 10^{-7}$	$\Delta m_D;  q/p , \phi_D$
$(\bar{c}_R u_L)(\bar{c}_L u_R)$	$6.2 \times 10^3$	$1.5 \times 10^4$	$5.7 \times 10^{-8}$	$1.1 \times 10^{-8}$	$\Delta m_D;  q/p , \phi_D$
$(\bar{b}_L \gamma^\mu d_L)^2$	$6.6 \times 10^2$	$9.3 \times 10^2$	$2.3 \times 10^{-6}$	$1.1 \times 10^{-6}$	$\Delta m_{B_d}; S_{\psi K_S}$
$(\bar{b}_R d_L)(\bar{b}_L d_R)$	$2.5 \times 10^3$	$3.6 \times 10^3$	$3.9 \times 10^{-7}$	$1.9 \times 10^{-7}$	$\Delta m_{B_d}; S_{\psi K_S}$
$(\bar{b}_L \gamma^\mu s_L)^2$	$1.4 \times 10^2$	$2.5 \times 10^2$	$5.0 \times 10^{-5}$	$1.7 \times 10^{-5}$	$\Delta m_{B_s}; S_{\psi\phi}$
$(\bar{b}_R s_L)(\bar{b}_L s_R)$	$4.8 \times 10^2$	$8.3 \times 10^2$	$8.8 \times 10^{-6}$	$2.9 \times 10^{-6}$	$\Delta m_{B_s}; S_{\psi\phi}$

**Table 1.** Bounds on some  $\Delta F = 2$  operators of the form  $(C/\Lambda^2)\mathcal{O}$ , with  $\mathcal{O}$  given in the first column. The bounds on  $\Lambda$  assume  $C = 1$ , the bounds on  $C$  assume  $\Lambda = 1$  TeV. (From Ref. [7].)

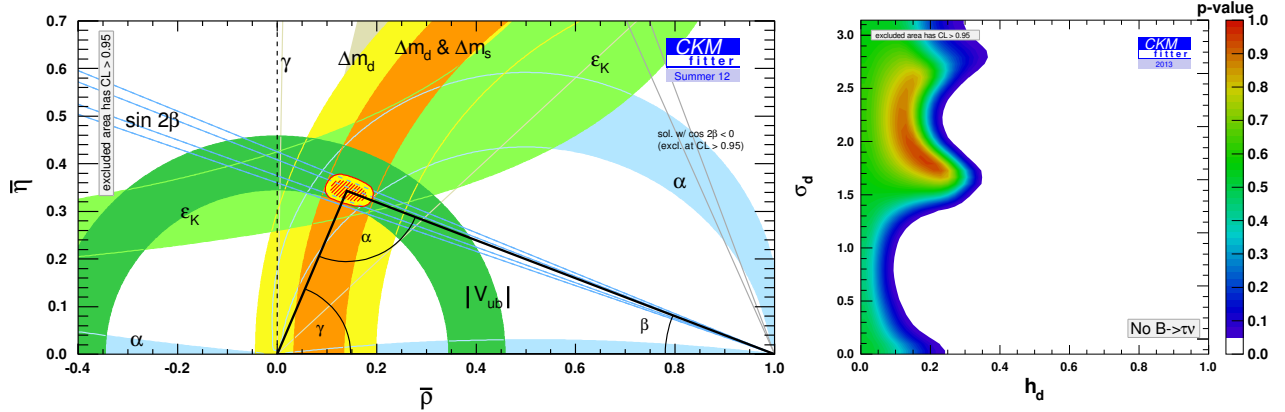


**Figure 1.** Left: Constraints on the apex of the unitarity triangle in the  $\bar{\rho} - \bar{\eta}$  plane (at 95% CL) [8, 9]. Right: the allowed  $h_d - \sigma_d$  new physics parameter space (see text) in  $B^0 - \bar{B}^0$  mixing.

use the Wolfenstein parameterization [10] of the CKM matrix (for a review, see [11]),

$$V_{\text{CKM}} = \begin{pmatrix} V_{ud} & V_{us} & V_{ub} \\ V_{cd} & V_{cs} & V_{cb} \\ V_{td} & V_{ts} & V_{tb} \end{pmatrix} = \begin{pmatrix} 1 - \frac{1}{2}\lambda^2 & \lambda & A\lambda^3(\bar{\rho} - i\bar{\eta}) \\ -\lambda & 1 - \frac{1}{2}\lambda^2 & A\lambda^2 \\ A\lambda^3(1 - \bar{\rho} - i\bar{\eta}) & -A\lambda^2 & 1 \end{pmatrix} + \mathcal{O}(\lambda^4). \quad (1)$$

It exhibits the hierarchical structure of the CKM matrix by expanding in a small parameter,  $\lambda \simeq 0.23$ . The unitarity of this matrix in the SM implies many relations, such as that defining the “unitarity triangle” shown in Fig. 1, which arises from rescaling  $V_{ud}V_{ub}^* + V_{cd}V_{cb}^* + V_{td}V_{tb}^* = 0$  by  $V_{cd}V_{cb}^*$  and choosing two vertices of the resulting triangle to be  $(0, 0)$  and  $(1, 0)$ .

As a result of second-order weak interaction processes, there are transitions between the neutral meson flavor eigenstates, so the physical mass eigenstates are their linear combinations, denoted as  $|B_{H,L}\rangle = p|B^0\rangle \mp q|\bar{B}^0\rangle$ . (The  $p$  and  $q$  parameters differ for the four neutral mesons, but the same notation is commonly used without distinguishing indices.) In a large class of models, the BSM physics modifies the mixing amplitude of neutral mesons, and leaves tree-level decays unaffected. This effect can be parameterized by just two real parameters for each mixing amplitude. For  $B^0 - \bar{B}^0$  mixing, writing  $M_{12} = M_{12}^{\text{SM}}(1 + h_d e^{2i\sigma_d})$ , the constraints on  $h_d$

and  $\sigma_d$  are shown in the right plot in Fig. 1. (Evidence for  $h_d \neq 0$  would rule out the SM.) Only in 2004, after the first significant constraints on  $\gamma$  and  $\alpha$  from *BABAR* and *Belle*, did we learn that the BSM contribution to  $B^0-\bar{B}^0$  mixing must be less than the SM amplitude [12, 9]. The right plot in Fig. 1 shows that order 20% corrections to  $|M_{12}|$  are still allowed for (almost) any value of the phase of the new physics contribution, and if this phase is aligned with the SM ( $\sigma_d = 0 \bmod \pi/2$ ), then the new physics contribution does not yet have to be much smaller than the SM one. Similar conclusions apply for  $B_s^0$  and  $K^0$  mixings [13, 14], as well as many other  $\Delta F = 1$  FCNC transition amplitudes.

The fact that such large deviations from the SM are not yet excluded gives very strong motivations to continue flavor physics measurements in order to observe deviations from the SM predictions or establish an even stronger hierarchy between the SM and new physics contributions.

In considering the future program, the following issues [15] are of key importance:

1. What are the expected deviations from the SM predictions induced by new physics at the TeV scale?  
As explained above, TeV-scale new physics with generic flavor structure is ruled out by many orders of magnitude. However, sizable deviations from the SM are still allowed by the current bounds, and in many scenarios observable effects are expected.
2. What are the theoretical uncertainties?  
These are highly process dependent. Some measurements are limited by theoretical uncertainties (due to hadronic, strong interaction, effects), but in many key processes the theory uncertainties are very small, below the expected sensitivity of future experiments.
3. In which processes will the sensitivity to BSM physics increase the most?  
The useful data sets can increase by a factor of order 100 (in most cases 10–1000), and will probe effects predicted by fairly generic BSM scenarios.
4. What will the measurements reveal, if deviations from the SM are [not] seen?  
The flavor physics data will be complementary with the high- $p_T$  part of the LHC program. The synergy of measurements can reveal a lot about what the new physics at the TeV scale is, and what it is not.

This report concentrates on the physics and prospects of a subset of measurements, for which the answers to these questions are the clearest, both in terms of theoretical cleanliness and experimental feasibility. The experiments will enable many additional measurements which are not discussed here, some due to lack of space, and some because they will be more important than can now be anticipated. (Recall that the best measurements of the CKM angles  $\alpha$  and  $\gamma$  at *BABAR* and *Belle* were not in formerly expected decay modes.) While future theory progress is important, the value of more sensitive experiments is not contingent on it.

## 2.2 The Role of Theory

To find a convincing deviation from the SM, a new physics effect has to be several times larger than the experimental uncertainty of the measurement and the theoretical uncertainty of the SM prediction. One often distinguishes two kinds of theoretical uncertainties, perturbative and nonperturbative (this separation is not unambiguous). Perturbative uncertainties come from the truncation of expansions in small (or not-so-small) coupling constants, such as  $\alpha_s$  at a few GeV scale. There are always higher order terms that have not been computed. Nonperturbative effects arise because QCD becomes strongly interacting at low energies, and these are often the limiting uncertainties. There are, nevertheless, several possibilities to get at the fundamental physics in certain cases.

- For some observables the hadronic parameters (mostly) cancel, or can be extracted from data (e.g., using the measured  $K \rightarrow \pi \ell \nu$  form factor to predict  $K \rightarrow \pi \nu \bar{\nu}$ , several methods to extract  $\gamma$ , etc.).



- In many cases, CP invariance of the strong interaction implies that the dominant hadronic physics cancels, or is CKM suppressed (e.g., measuring  $\beta$  from  $B \rightarrow \psi K_S$ , and some other CP asymmetries).
- In some cases one can use symmetries of the strong interaction which arise in certain limits, such as the chiral or the heavy quark limit, to establish that nonperturbative effects are suppressed by small parameters, and to estimate or extract them from data (e.g., measuring  $|V_{us}|$  and  $|V_{cb}|$ , inclusive rates).
- Lattice QCD is a model-independent method to address nonperturbative phenomena. The most precise results to date are for matrix elements involving at most one hadron in the initial and the final state (allowing, e.g., extractions of magnitudes of CKM elements).

All of these approaches use experimental data from related processes to fix some parameters, constrain the uncertainties, and cross-check the methods. Thus, experimental progress on a broad program will not only reduce the uncertainties of key measurements, but also help reduce theoretical uncertainties.

As an example, consider extracting  $\gamma$  from  $B \rightarrow DK$ . This is one of the cleanest measurements in terms of theoretical uncertainties, because all the necessary hadronic quantities can be measured. All  $B \rightarrow DK$  based analyses consider decays of the type  $B \rightarrow D^0(\bar{D}^0) K(X) \rightarrow F_D K(X)$ , where  $F_D$  is a final state that is accessible in both  $D^0$  and  $\bar{D}^0$  decay, allowing for interference, and  $X$  represents possible extra particles in the final state. Using several  $B \rightarrow DKX$  decay modes (say,  $n$  different  $X$  states and  $k$  different  $D^0$  and  $\bar{D}^0$  decay modes), one can perform  $nk$  measurements, which depend on  $n+k$  decay amplitudes. Thus, one can determine all hadronic parameters, as well as the weak phase  $\gamma$ , with very little theoretical uncertainty.

The main reason why many CP asymmetry measurements have small theoretical uncertainties is because they involve ratios of rates, from which the leading amplitudes cancel, so the uncertainties are suppressed by the relative magnitude of the subleading amplitudes. This is the case for the time dependent CP asymmetry in  $B \rightarrow \psi K_S$ , in which case the subdominant amplitude is suppressed by a factor  $\sim 50$  due to CKM elements and by the ratio of the matrix element of a loop diagram compared to a tree diagram. However, it is not simple to precisely quantify the uncertainties below the percent level. In other modes (e.g.,  $B \rightarrow \phi K_S$ ,  $\eta' K_S$ , etc.) the loop suppression of the hadronic uncertainty is absent, and the theoretical understanding directly impacts at what level new physics can be unambiguously observed.

Symmetries of the strong interaction that occur for hadrons containing light quarks ( $m_{u,d,s} < \Lambda_{\text{QCD}}$ ) or for hadrons containing a heavy quark ( $m_{b,c} > \Lambda_{\text{QCD}}$ ) have played critical roles in understanding flavor physics. Chiral perturbation theory has been very important for kaon physics, and isospin symmetry is crucial for the determination of  $\alpha$  in  $B \rightarrow \pi\pi$ ,  $\rho\rho$ , and  $\rho\pi$  decays. For  $B$  and  $D$  mesons, extra symmetries of the Lagrangian emerge in the  $m_{b,c} \gg \Lambda_{\text{QCD}}$  limit, and these heavy quark spin-flavor symmetries imply, for example, that exclusive semileptonic  $B \rightarrow D^{(*)}\ell\bar{\nu}$  decays are described by a single universal Isgur-Wise function in the symmetry limit. For inclusive semileptonic  $B$  decays, an operator product expansion can be used to compute sufficiently inclusive rates; applications include the extraction of  $|V_{cb}|$ . As is often the case, after understanding the symmetry limit and its implications, it is the analysis of subleading effects where many theoretical challenges lie. The theoretical tools to make further progress are well-developed, but much work remains to be done to reach the ultimate sensitivities.

Lattice QCD has become an important tool in flavor physics, and significant improvements are expected. As substantial investment in computational infrastructure is required, a separate section discusses it in this report. Lattice QCD allows first-principles calculations of some nonperturbative phenomena. In practice, approximations have to be made due to finite computing power, which introduce systematic uncertainties that can be studied (e.g., dependence on lattice spacing, spatial volume, etc.). Due to new algorithms and more powerful computers, matrix elements which contain at most one hadron in the final state should soon be calculable with percent level uncertainties. Matrix elements involving states with sizable widths, e.g.,  $\rho$  and  $K^*$ , are more challenging. So are calculations of matrix elements containing more than one hadron in

Observable	SM Theory	Current Expt.	Future Experiments
$\mathcal{B}(K^+ \rightarrow \pi^+ \nu \bar{\nu})$	$7.81(75)(29) \times 10^{-11}$	$1.73_{-1.05}^{+1.15} \times 10^{-10}$ E787/E949	$\sim 10\%$ at NA62 $\sim 5\%$ at ORKA $\sim 2\%$ at <i>Project X</i>
$\mathcal{B}(K_L^0 \rightarrow \pi^0 \nu \bar{\nu})$	$2.43(39)(6) \times 10^{-11}$	$< 2.6 \times 10^{-8}$ E391a	1 <sup>st</sup> observation at KOTO $\sim 5\%$ at <i>Project X</i>
$\mathcal{B}(K_L^0 \rightarrow \pi^0 e^+ e^-)$	$(3.23_{-0.79}^{+0.91}) \times 10^{-11}$	$< 2.8 \times 10^{-10}$ KTeV	$\sim 10\%$ at <i>Project X</i>
$\mathcal{B}(K_L^0 \rightarrow \pi^0 \mu^+ \mu^-)$	$(1.29_{-0.23}^{+0.24}) \times 10^{-11}$	$< 3.8 \times 10^{-10}$ KTeV	$\sim 10\%$ at <i>Project X</i>
$ P_T $ in $K^+ \rightarrow \pi^0 \mu^+ \nu$	$\sim 10^{-7}$	$< 0.0050$	$< 0.0003$ at TREK $< 0.0001$ at <i>Project X</i>
$\Gamma(K_{e2})/\Gamma(K_{\mu 2})$	$2.477(1) \times 10^{-5}$	$2.488(10) \times 10^{-5}$ (NA62, KLOE)	$\pm 0.0054 \times 10^{-5}$ at TREK $\pm 0.0025 \times 10^{-5}$ at <i>Project X</i>
$\mathcal{B}(K_L^0 \rightarrow \mu^\pm e^\mp)$	$< 10^{-25}$	$< 4.7 \times 10^{-12}$	$< 2 \times 10^{-13}$ at <i>Project X</i>

**Table 2.** A summary of the reach of current and proposed experiments for some key rare kaon decay measurements, in comparison to standard model theory and the current best experimental results. In the SM predictions for the  $K \rightarrow \pi \nu \bar{\nu}$  and  $K \rightarrow \pi \ell^+ \ell^-$  the first error is parametric, the second denotes the intrinsic theoretical uncertainty.

the final state, and it will require further developments to obtain small uncertainties for those. Thus, lattice QCD errors are expected to become especially small for leptonic and semileptonic decays, and meson mixing.

In summary, there are many observables with theoretical uncertainties at the few percent level, matching the expected experimental sensitivity, which is necessary to allow a discovery of small new physics contributions. The full exploitation of the experimental program requires continued support of theoretical developments.

### 3 Report of the Kaon Task Force

Kaon decays have played a pivotal role in shaping the standard model (SM). Prominent examples include the introduction of internal “flavor” quantum numbers (strangeness), parity violation ( $K \rightarrow 2\pi, 3\pi$  puzzle), quark mixing, meson-antimeson oscillations, discovery of CP violation, suppression of flavor-changing neutral currents (FCNC), discovery of the GIM (Glashow-Iliopoulos-Maiani) mechanism and prediction of charm. Now and looking ahead, kaons continue to have high impact in constraining the flavor sector of possible extensions of the SM.

In the arena of kaon decays, a key role is played by the FCNC modes mediated by the quark-level processes  $s \rightarrow d(\gamma, \ell^+ \ell^-, \nu \bar{\nu})$ , and in particular the four theoretically cleanest modes  $K^+ \rightarrow \pi^+ \nu \bar{\nu}$ ,  $K_L \rightarrow \pi^0 \nu \bar{\nu}$ ,  $K_L \rightarrow \pi^0 e^+ e^-$ ,  $K_L \rightarrow \pi^0 \mu^+ \mu^-$ . Because of the peculiar suppression of the SM amplitude (top-quark loop suppressed by  $|V_{td}V_{ts}| \sim \lambda^5$ ) which in general is not present in SM extensions, kaon FCNC modes offer a unique window on the flavor structure of such extensions. This argument by itself provides a strong and model-independent motivation to study these modes in the LHC era. Rare kaon decays can elucidate the flavor structure of SM extensions, information that is in general not accessible from high-energy colliders.

The actual “discovery potential” depends on the precision of the prediction for these decays in the SM, the level of constraints from other observables, and how well we can measure their branching ratios.

### 3.1 Rare Kaon Decays in the Standard Model: Status and Forecast

State-of-the-art predictions (see Ref. [16] and references therein) are summarized in Table 2 along with current and expected experimental results. The predictions show our current knowledge of the theoretical branching ratio uncertainties:  $K^+ \rightarrow \pi^+ \nu \bar{\nu}$  at the 10% level,  $K_L \rightarrow \pi^0 \nu \bar{\nu}$  at the 15% level, and  $K_L \rightarrow \pi^0 e^+ e^-$  and  $K_L \rightarrow \pi^0 \mu^+ \mu^-$  at the 25–30% level. In the neutrino modes, the intrinsic theoretical uncertainty is a small fraction of the total, which is currently dominated by the uncertainty in CKM parameters. In the charged lepton modes, the uncertainty is dominated by long distance contributions which can be parametrized in terms of the rates of other decays (such as  $K_S \rightarrow \pi^0 \ell^+ \ell^-$ ). It is expected that in the next decade progress in lattice QCD and in  $B$  meson measurements (LHCb and Belle II) will reduce the uncertainty on both  $K \rightarrow \pi \nu \bar{\nu}$  modes to the 5% level. Substantial improvements in  $K_L \rightarrow \pi^0 \ell^+ \ell^-$  will have to rely on lattice QCD computations, requiring evaluation of bi-local operators. Exploratory steps exist, but involve new techniques, making it hard to forecast the level of uncertainty that can be achieved. Therefore, from a theory perspective, the golden modes remain the  $K \rightarrow \pi \nu \bar{\nu}$  decays, because they have small long-distance contamination (negligible in the CP-violating  $K_L$  mode). The  $K \rightarrow \pi \nu \bar{\nu}$  decay rates, especially in the  $K_L$  mode, can be predicted with smaller theoretical uncertainties than other FCNC decay rates involving quarks.

### 3.2 Beyond the Standard Model Physics Reach

The beyond the standard model (BSM) reach of rare FCNC kaon decays has received significant attention in the literature, through both explicit model analyses and model-independent approaches based on effective field theory (EFT). In the absence of a clear candidate for the TeV extension of the SM, the case for discovery potential and model-discriminating power can be presented very efficiently in terms of an EFT approach to BSM physics. In this approach, one parametrizes the effects of new heavy particles in terms of local operators whose coefficients are suppressed by inverse powers of the heavy new physics mass scale. The important point is that the EFT approach allows us to make statements that apply to classes of models, not just any specific SM extension. In this context, one can ask two important questions: (i) how large a deviation from the SM can we expect in rare decays from existing constraints? (ii) if a given class of operators dominates, what pattern of deviations from the SM can we expect in various rare kaon decays?

Our discussion here parallels the one given in Ref. [18], to which we refer for more details. To leading order in  $v/\Lambda$  (where  $v \sim 200$  GeV and  $\Lambda$  is the scale of new physics), six operators can affect the  $K \rightarrow \pi \nu \bar{\nu}$  decays. Three of these are four-fermion operators and affect the  $K \rightarrow \pi \ell^+ \ell^-$  decays as well (one of these operators contributes to  $K \rightarrow \pi \ell \nu$  by  $SU(2)$  gauge invariance). The coefficients of these operators are largely unconstrained by other observables, and therefore one can expect sizable deviations from the SM in  $K \rightarrow \pi \nu \bar{\nu}$  (both modes) and  $K \rightarrow \pi \ell^+ \ell^-$ , depending on the flavor structure of the BSM scenario.

The other three leading operators contributing to  $K \rightarrow \pi \nu \bar{\nu}$  involve the Higgs field and reduce, after electroweak symmetry breaking, to effective flavor-changing  $Z$ -boson interactions, with both left-handed (LH) and right-handed (RH) couplings to quarks. These “ $Z$ -penguin” operators (both LH and RH) are the leading effect in many SM extensions, and affect a large number of kaon observables ( $K \rightarrow \pi \ell^+ \ell^-$ ,  $\epsilon_K$ ,  $\epsilon'_K/\epsilon_K$ , and in the case of one operator  $K \rightarrow \pi \ell \nu$  through  $SU(2)$  gauge invariance). Focusing on this class of operators, the relevant part of the effective Lagrangian reads

$$\mathcal{L}_{\text{eff}} \propto (\lambda_t C_{\text{SM}} + C_{\text{NP}}) \bar{d}_L \gamma_\mu s_L Z^\mu + \tilde{C}_{\text{NP}} d_R \gamma_\mu s_R Z^\mu, \quad (2)$$

where  $\lambda_q = V_{qs}^* V_{qd}$  with  $V_{ij}$  denoting elements of the CKM matrix, and  $C_{\text{SM}} \approx 0.8$  encodes the SM contribution to the LH  $Z$ -penguin (the RH  $Z$ -penguin is highly suppressed in the SM by small quark

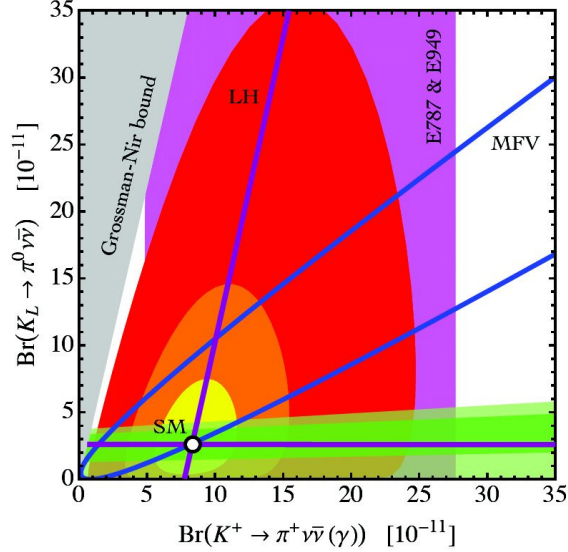


**Figure 2.** Predictions for the  $K \rightarrow \pi \nu \bar{\nu}$  branching ratios assuming dominance of the  $Z$ -penguin operators, for different choices of the effective couplings  $C_{\text{NP}}, \tilde{C}_{\text{NP}}$  [24]. The SM point is indicated by a white dot with black border. The yellow, orange, and red shaded contours correspond to  $|C_{\text{NP}}, \tilde{C}_{\text{NP}}| \leq \{0.5, 1, 2\} |\lambda_t C_{\text{SM}}|$ , the magenta band indicates the 68% confidence level (CL) constraint on  $\mathcal{B}(K^+ \rightarrow \pi^+ \nu \bar{\nu}(\gamma))$  from experiment [25], and the gray area is theoretically inaccessible [26]. The blue parabola represents the subspace accessible to MFV models. The purple straight lines represent the subspace accessible in models that have only LH currents, due to the constraint from  $\epsilon_K$  [27]. The green band represents the region accessible after taking into account the correlation of  $K_L \rightarrow \pi^0 \nu \bar{\nu}$  with  $\epsilon'_K/\epsilon_K$ : the (light) dark band corresponds to predictions of  $\epsilon'_K/\epsilon_K$  within a factor of (5) 2 of the experimental value, using central values for the hadronic matrix elements as reported in [20] and references therein.

masses). Assuming dominance of the  $Z$ -penguin operators, one can study the expectations for the  $K \rightarrow \pi \nu \bar{\nu}$  branching ratio for different choices of the effective couplings  $C_{\text{NP}}, \tilde{C}_{\text{NP}}$ , and address the correlations with other observables. This is illustrated in Fig. 2. In this framework,  $\epsilon'_K/\epsilon_K$  provides the strongest constraint on the CP violating mode  $K_L \rightarrow \pi^0 \nu \bar{\nu}$  [19, 20, 21, 22, 23]. This is illustrated by the green bands in Fig. 2, where one can see that the requirement  $\epsilon'_K/\epsilon_K \in [0.2, 5](\epsilon'_K/\epsilon_K)_{\text{exp}}$  limits deviations in the  $K_L \rightarrow \pi^0 \nu \bar{\nu}$  to be of  $\mathcal{O}(1)$ , while leaving room for larger deviations in the CP conserving mode  $K^+ \rightarrow \pi^+ \nu \bar{\nu}$ . The correlation between  $\epsilon'_K/\epsilon_K$  and  $K_L \rightarrow \pi^0 \nu \bar{\nu}$  can be evaded only if there is a cancellation among the  $Z$ -penguin and other contributions to  $\epsilon'_K/\epsilon_K$ . Moreover, we stress that this conclusion holds in all models in which the  $Z$ -penguin provides the dominant contribution to  $K \rightarrow \pi \nu \bar{\nu}$  decays. While this is not true in general, we think this constraint should be one of the drivers of the design sensitivity for  $K_L \rightarrow \pi^0 \nu \bar{\nu}$  experiments.

The number of operators that affect the  $K_L \rightarrow \pi^0 \ell^+ \ell^-$  ( $\ell = e, \mu$ ) decays is larger than the case of  $K \rightarrow \pi \nu \bar{\nu}$ . Besides (axial-)vector operators resulting from  $Z$ - and photon-penguin diagrams, (pseudo-)scalar operators associated with Higgs exchange can play a role [28]. In a model-independent framework:

$$\mathcal{L}_{\text{eff}} \supset C_A Q_A + C_V Q_V + C_P Q_P + C_S Q_S, \quad (3)$$

with

$$Q_A = (\bar{d} \gamma^\mu s)(\bar{\ell} \gamma_\mu \gamma_5 \ell), \quad Q_V = (\bar{d} \gamma^\mu s)(\bar{\ell} \gamma_\mu \ell), \quad Q_P = (\bar{d} s)(\bar{\ell} \gamma_5 \ell), \quad Q_S = (\bar{d} s)(\bar{\ell} \ell). \quad (4)$$

In Figure 3 we depict the accessible parameter space corresponding to various classes of NP. The blue parabola illustrates again the predictions obtained by allowing only for a contribution  $C_{\text{NP}}$  with arbitrary modulus and phase. We see that in models with dominance of the LH  $Z$ -penguin the deviations in  $K_L \rightarrow \pi^0 \ell^+ \ell^-$

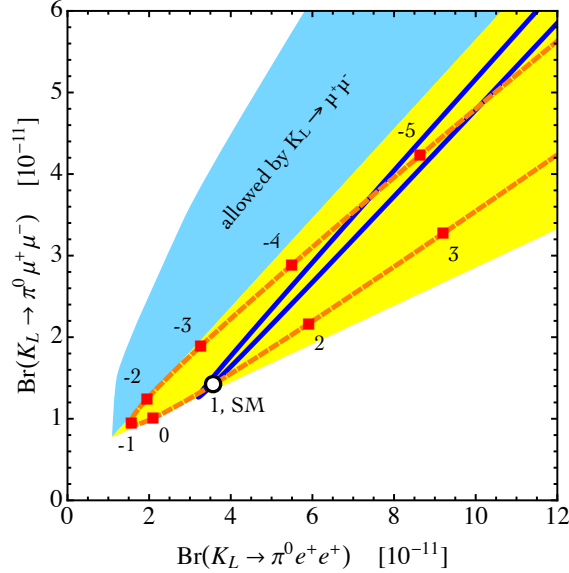


**Figure 3.** Predictions for the  $K_L \rightarrow \pi^0 \ell^+ \ell^-$  branching ratios assuming different types of NP contributions [24]. The SM point is indicated by a white dot with black border. The blue parabola represents the region accessible by allowing only for  $C_{NP}$  with arbitrary modulus and phase. The subspace accessible when  $C_{V,A} \neq 0$  is represented by the dashed orange parabola (common rescaling of  $C_{A,V}$ ) and the yellow shaded region (arbitrary values of  $C_{A,V}$ ). The subspace accessible when  $C_{S,P} \neq 0$  (compatibly with  $K_L \rightarrow \mu^+ \mu^-$ ) is represented by the light blue shaded region.

are strongly correlated. A large photon-penguin can induce significant corrections in  $C_V$ , which breaks this correlation and opens up the parameter space as illustrated by the dashed orange parabola and the yellow shaded region. The former predictions are obtained by employing a common rescaling of  $C_{A,V}$ , while in the latter case the coefficients  $C_{A,V}$  are allowed to take arbitrary values. If besides  $Q_{A,V}$ ,  $Q_{P,S}$  can also receive sizable NP corrections, then a further relative enhancement of  $\text{Br}(K_L \rightarrow \pi^0 \mu^+ \mu^-)$  compared to  $\text{Br}(K_L \rightarrow \pi^0 e^+ e^-)$  is possible. This feature is exemplified by the light blue shaded region that corresponds to the parameter space that is compatible with the constraints on  $C_{P,S}$  arising from  $K_L \rightarrow \mu^+ \mu^-$ . Finally, we note that  $K_L \rightarrow \mu^+ \mu^-$  itself is another FCNC mode of interest, as it is sensitive to different combinations of new physics couplings. The constraining power of  $K_L \rightarrow \mu^+ \mu^-$  is limited by the current understanding of the dispersive part of the amplitude. Despite this, the mode already provides useful diagnostic power, as in combination with  $K \rightarrow \pi \nu \bar{\nu}$  can help distinguish among LH or RH coupling of  $Z$  and  $Z'$  to quarks [29, 30, 31].

Rare kaon decays have been extensively studied within well motivated extensions of the SM, such as supersymmetry (SUSY) [32] and warped extra dimensions (Randall-Sundrum) models [20, 29]. In all cases, deviations from the SM can be sizable and perhaps most importantly the correlations between various rare  $K$  decays are essential in discriminating among models. Rare  $K \rightarrow \pi \nu \bar{\nu}$  experiments can also probe the existence of light states very weakly coupled to the SM appearing in various dark sector models [33], through the experimental signature  $K \rightarrow \pi +$  (missing energy) and distortions to the pion spectrum.

### Other modes

Besides the FCNC modes, kaon decays also provide exquisite probes of the charged-current sector of SM extensions, probing scales of TeV or above. Theoretically, the cleanest probes are (i) the ratio  $R_K \equiv$

$\Gamma(K \rightarrow e\nu)/\Gamma(K \rightarrow \mu\nu)$ , which tests lepton universality, scalar, and tensor charged-current interactions; (ii) the transverse muon polarization  $P_\mu^T$  in the semi-leptonic decay  $K^+ \rightarrow \pi^0\mu^+\nu_\mu$ , which is sensitive to BSM sources of CP violation in scalar charged-current operators. In both cases there is a clean discovery window provided by the precise SM theoretical prediction [34] ( $R_K$ ) and by the fact that in the SM  $P_\mu^T$  is generated only by very small and known final state interactions [35]. Table 2 provides a summary of SM predictions for these processes, along with current and projected experimental sensitivities at ongoing or planned experiments.

### 3.3 Experimental Program

Following the termination of a world-class kaon program in the U.S. by 2002, leadership in kaon physics shifted to Europe and Japan, where a program of experiments aiming for orders of magnitude improvements in reach for new physics is now in progress.

The NA62 experiment at CERN [36] uses, for the first time, the in-flight technique to search for  $K^+ \rightarrow \pi^+\nu\bar{\nu}$ . NA62 will finish commissioning at the end of 2013 and start physics running toward the end of 2014. The NA62 goal is to measure the  $K^+ \rightarrow \pi^+\nu\bar{\nu}$  branching ratio with 10% precision along with a robust and diverse kaon physics program.

The KOTO experiment at JPARC [37] is an in-flight measurement of  $K_L^0 \rightarrow \pi^0\nu\bar{\nu}$ . Significant experience and a better understanding of the backgrounds were obtained in its predecessor, E391a. The anticipated experimental sensitivity is a few SM signal events in three years of running with 300 kW of beam power. Commissioning runs were undertaken in 2012 and 2013 and physics running started in 2013, but the longer term performance of the experiment will depend upon beam power evolution of the JPARC accelerator.

The TREK experiment at JPARC [38] will search for T violation in stopped charged kaon decays by measuring the polarization asymmetry in  $K^+ \rightarrow \pi^0\mu^+\nu_\mu$  decays. TREK needs at least 100 kW (the proposal assumed 270 kW) for this measurement. While the accelerator is running at lower power, collaborators have proposed a search for lepton flavor universality violation through the measurement of  $\Gamma(K \rightarrow e\nu)/\Gamma(K \rightarrow \mu\nu)$  at the 0.2% level, which will use much of the TREK apparatus and requires only 30 kW of beam power and will be ready to run in 2015. At the same time, this configuration allows for sensitive searches for a heavy sterile neutrino ( $N$ ) in  $K^+ \rightarrow \mu^+N$ , and for light bosons (heavy photons from the dark sector,  $A' \rightarrow e^+e^-$ ) in the  $K^+ \rightarrow \mu^+\nu_\mu e^+e^-$  and  $K^+ \rightarrow \pi^+e^+e^-$  decays, where the new particles would be identified as narrow peaks in the respective momentum and  $e^+e^-$  invariant mass spectra. The uncertainty of the JPARC beam power profile and potential conflicts for beamline real estate make the long term future of the TREK experiment unclear.

The KLOE-2 experiment [39] will extend the results of KLOE to improve neutral kaon interference measurements, CPT and quantum mechanics tests, and a wide range of measurements of non-leptonic and radiative kaon decays.

The ORKA experiment is proposed to measure  $K^+ \rightarrow \pi^+\nu\bar{\nu}$  with 1000 event sensitivity at the Fermilab Main Injector (MI) [40]. After a five year run ORKA will reach a precision of 5% on the branching ratio, which is the expected level of theoretical precision. This high-precision measurement would be one of the most incisive probes of quark flavor physics in the coming decade. ORKA is a stopped kaon experiment that builds on the experience of the E787/949 experiments at Brookhaven that observed seven candidate events. Backgrounds, primarily from other kaon decays at branching fractions as much as 10 orders of magnitude larger, have similar signatures to the signal. ORKA takes advantage of the extensive knowledge of background rates and characteristics from E787/E949 by using the same proven experimental techniques. The methods

for suppressing backgrounds are well known, as are the background rates and experimental acceptance. Improvements in detector performance are possible due to significant advances in detector technology in the 25 years since E787 first ran. The new ORKA detector with beam supplied by the MI running at 95 GeV with moderate duty factor presents an opportunity to extend the E787/E949 approach by two orders of magnitude in sensitivity. The first order of magnitude improvement comes from the substantially brighter source of low energy kaons and the second arises from incremental improvements to the experimental techniques firmly established at BNL. ORKA will observe 210 SM events per year and will make a wide variety of measurements in addition to the  $K^+ \rightarrow \pi^+ \nu \bar{\nu}$  mode. ORKA will search for and study a range of important reactions involving kaon and pion decays, such as tests of lepton universality, symmetry violations, hidden sector particles, heavy neutrinos and other topics. ORKA will be a world-leading kaon physics experiment, train a new generation of kaon physicists and position the U.S. to move forward to a *Project X* kaon program. It is an essential step in developing a robust intensity frontier program in the U.S. at *Project X*.

The U.S. has an opportunity through ORKA to re-establish a leadership position in kaon physics.

### ***Project X***

A flagship experiment of the *Project X* physics program will measure the  $K_L^0 \rightarrow \pi^0 \nu \bar{\nu}$  branching ratio with 5% precision. This effort will build on the KOTO experience, benefit from the KOPIO initiative [41], and take advantage of the beam power and flexibility provided by Stage 2 of *Project X*.

KOPIO proposed to measure  $K_L^0 \rightarrow \pi^0 \nu \bar{\nu}$  with a SM sensitivity of 100 events at the BNL Alternating Gradient Synchrotron (AGS) as part of the RSVP (Rare Symmetry Violating Processes) project. The experimental technique and sensitivity were well-developed and extensively reviewed. KOPIO was designed to use a neutral beam at a  $42^\circ$  targeting angle produced by 24 GeV protons from the AGS. The neutral kaons would have an average momentum of 800 MeV/ $c$  with a range of 300–1500 MeV/ $c$ . A low momentum beam was critical for the time-of-flight (TOF) strategy of the experiment.

The TOF technique is even better matched to the kaon momentum produced by the 3 GeV proton beam at *Project X* where the higher momentum tail present in the AGS beam is suppressed. Performance of the TOF strategy was limited by the design bunch width of 200 ps at the AGS. The *Project X* beam pulse timing, including target time slewing, is expected to be less than 50 ps and would substantially improve the momentum resolution and background rejection capability of the  $K_L^0 \rightarrow \pi^0 \nu \bar{\nu}$  experiment driven with the *Project X* beam.

The AGS  $K_L$  yield per proton is 20 times the *Project X* yield; however, the 0.5 mA *Project X* proton flux is 150 times the RSVP goal of  $10^{14}$  protons every 5 seconds. Hence the neutral kaon flux at *Project X* will be 8 times the AGS flux goal into the same beam acceptance. The *Project X* neutral beam will contain about a factor of three more neutrons, but neutron interactions will be highly suppressed by the evacuated beamline and detector volume. The nominal five-year *Project X* run is 2.5 times longer than the KOPIO initiative at the AGS and hence the reach of a *Project X*  $K_L^0 \rightarrow \pi^0 \nu \bar{\nu}$  experiment would be 20 times greater than RSVP.

A TOF-based  $K_L^0 \rightarrow \pi^0 \nu \bar{\nu}$  experiment driven by *Project X* would be re-optimized for the *Project X*  $K_L$  momentum spectrum, TOF resolution, and corresponding background rejection. It is likely that this optimization would result in a smaller neutral beam solid angle which would simplify the detector design, increase the acceptance and relax the requirement to tag photons in the fierce rate environment of the neutral beam. Optimizing the performance will probably require a proton pulse train frequency of 20–50 MHz and an individual proton pulse timing width of  $\sim 20$  ps. Based on the E391a and KOTO experience, a careful design of the target and neutral beam channel is required to minimize the neutron halo and to assure target survival in the intense proton beam. The high  $K_L$  beam flux and the potential of break-through improvements in

TOF performance and calorimeter technology support the viability of a  $K_L^0 \rightarrow \pi^0 \nu \bar{\nu}$  experiment with  $\sim 1000$  SM event sensitivity.

If ORKA [40] observes a significant non-SM result, the  $K^+ \rightarrow \pi^+ \nu \bar{\nu}$  decay mode could be studied with higher statistics with a  $K^+$  beam driven by *Project X*. The high-purity, low-momentum  $K^+$  beam designed for ORKA could also serve experiments to precisely measure the polarization asymmetry in  $K^+ \rightarrow \pi^0 \mu^+ \nu_\mu$  decays and to continue the search for lepton flavor universality violation through the measurement of  $\Gamma(K \rightarrow e\nu)/\Gamma(K \rightarrow \mu\nu)$  at high precision.

Depending upon the outcome of the TREK experiment at JPARC, a T violation experiment would be an excellent candidate for *Project X*, as would a multi-purpose experiment dedicated to rare modes that involve both charged and neutral particles in the final state. This experiment might be able to pursue  $K_L \rightarrow \pi^0 \ell^+ \ell^-$  as well as many other radiative and leptonic modes. The kaon physics program at *Project X* could be very rich indeed.

### 3.4 Conclusions

Kaon decays are extremely sensitive probes of the flavor and CP-violating sector of any SM extension. The  $K \rightarrow \pi \nu \bar{\nu}$  golden modes have great discovery potential: (i) sizable,  $\mathcal{O}(1)$ , deviations from the SM are possible; (ii) even small deviations can be detected due to the precise theoretical predictions. Next generation searches should aim for a sensitivity level of  $10^3$  SM events (few % uncertainty) in both  $K^+$  and  $K_L$  modes, in order to maximize discovery potential.

We foresee searches for both  $K \rightarrow \pi \nu \bar{\nu}$  modes as flagship measurements of a reinvigorated U.S.-led kaon program. As summarized in Table 2, through ORKA and *Project X* this program has the opportunity to pursue a broad set of measurements, exploring the full discovery potential and model-discrimination power of kaon physics.

## 4 Report of the *B*-Physics Task Force

### 4.1 Physics Motivation

#### Searches for BSM Physics

Rare *B* physics processes are sensitive to new physics (NP) because the heavy particles can contribute through virtual corrections to the effective weak Hamiltonian. This makes it possible, for example, to probe extended Higgs sectors and to test for the presence of new gauge interactions or for extended matter content such as the ones encountered in supersymmetric models. The sensitivity to NP depends on how large the flavor violating couplings are. For instance, in the most conservative case of Minimal Flavor Violation (MFV) with new particles only contributing in the loops, the rare *B* processes can probe mass scales of roughly  $\sim \mathcal{O}(\text{TeV})$  with the next generation experiments. In the case of general flavor violation with  $\mathcal{O}(1)$  off-diagonal couplings, on the other hand, one probes mass scales of  $\mathcal{O}(10^3 \text{ TeV})$  [1]. Because the dependence on new particle masses and (flavor-violating) couplings is different than in the on-shell production, the NP searches at LHCb and Belle II are also complementary to the high  $p_T$  NP searches at ATLAS and CMS.



Observables that are especially interesting for the future *B* physics program are those that have small or systematically improvable theoretical uncertainties. An important input is provided by measurements of the standard CKM unitarity triangle. The angle  $\gamma$  and modulus  $|V_{ub}|$  are determined from tree-level processes and thus less prone to contributions from NP. They provide the SM “reference” determination of the CKM unitarity triangle (in effect its apex, the values of  $\bar{\rho}$  and  $\bar{\eta}$ ).  $|V_{ub}|$  is measured from inclusive and exclusive  $b \rightarrow u\ell\nu$  processes. There is an on-going effort to improve the theory predictions using both the continuum methods and lattice QCD, and a factor of a few improvements on the errors seem feasible. For instance, the present theory error on  $|V_{ub}|$  from exclusive  $B \rightarrow \pi\ell\nu$  can be reduced from present 8.7% to 2% by 2018 [42] (see Table 6). The theoretical uncertainties in the measurement of  $\gamma$  from  $B \rightarrow DK$  decays are even smaller. All the required hadronic matrix elements can be measured, because of the cascade nature of the  $B \rightarrow DK$ ,  $D \rightarrow f$  decay, if enough final states  $f$  are taken into account. The irreducible theoretical errors thus enter only at the level of one-loop electroweak corrections and are below  $\mathcal{O}(10^{-6})$  [43]. The present experimental errors are  $\pm 12^\circ$  from the average of *BABAR* and *Belle* measurements. LHCb has recently matched this precision. The errors are statistics-limited and will be substantially decreased in the future.

The tree-level determinations of  $\bar{\rho}$  and  $\bar{\eta}$  can then be compared with the measurements from loop-induced FCNCs, for instance with the time-dependent CP asymmetry in  $B \rightarrow J/\psi K_S$  and related modes determining the angle  $\beta$ . With improved theoretical control BSM physics can be constrained or even discovered. NP could also enter in the  $B_s - \bar{B}_s$  mixing. In the SM the mixing phase is small, suppressed by  $\lambda^2$  compared to  $\beta$ . Thus, in the SM, the corresponding time-dependent CP asymmetry in the  $b \rightarrow c\bar{c}s$  dominated decays, such as  $B_s \rightarrow J/\psi\phi$ , is predicted very precisely,  $\beta_s^{(\text{SM})} = 0.0182 \pm 0.0008$ . The LHCb result,  $\beta_s = -0.035 \pm 0.045$  [44], is consistent with the SM expectation, but the statistical uncertainty is much greater than that of the SM prediction. Since the uncertainty of the SM prediction is very small, future significant improvements of the measurement of  $\beta_s$  will directly translate to a better sensitivity to BSM physics.

Another important search for NP is to compare the time-dependent CP asymmetries of penguin-dominated  $b \rightarrow q\bar{q}s$  processes with the tree dominated  $b \rightarrow c\bar{c}s$  decays. Observables that probe this are the differences of CP asymmetries  $S_{J/\psi K_S} - S_{\phi K_S}$ ,  $S_{\psi K_S} - S_{\eta' K_S}$ , etc., in  $B_d$  decay, and  $S_{J/\psi\phi} - S_{\phi\phi}$  in  $B_s$  decay.

The list of interesting observables in *B* physics is very long. One could emphasize in particular the rare *B* decays with leptons in the final state. The  $B_s \rightarrow \ell^+\ell^-$  decay is especially interesting for SUSY searches in view of the fact that these are  $(\tan\beta)^6$  enhanced. LHCb presented first evidence of this decay, with  $\mathcal{B}(B_s \rightarrow \mu^+\mu^-) = (3.2_{-1.2}^{+1.5}) \times 10^{-9}$  [45] consistent with the SM prediction  $(3.54 \pm 0.30) \times 10^{-9}$  [46, 47]. Also, CMS has very recently reported a measurement of  $\mathcal{B}(B_s \rightarrow \mu^+\mu^-) = (3.0_{-0.9}^{+1.0}) \times 10^{-9}$  [48] consistent with the earlier LHCb result, and LHCb has also updated its value to  $\mathcal{B}(B_s \rightarrow \mu^+\mu^-) = (2.9_{-1.0}^{+1.1}) \times 10^{-9}$  [49]. This puts strong constraints on the large  $\tan\beta$  region of MSSM, favored by the measured Higgs mass for the case of TeV scale squarks. The theoretical errors on the SM prediction are still several times smaller than the experimental ones, making more precise measurements highly interesting. With the LHCb upgrade, the search for  $B_d \rightarrow \ell^+\ell^-$  will also get near the SM level. Rare decays involving a  $\nu\bar{\nu}$  pair are theoretically very clean, and *Belle II* should reach the SM level in  $B \rightarrow K^{(*)}\nu\bar{\nu}$ ; the current constraints are an order of magnitude weaker. There is also a long list of interesting measurements in  $b \rightarrow s\gamma$  and  $b \rightarrow s\ell^+\ell^-$  mediated inclusive and exclusive decays, CP asymmetries, angular distributions, triple product correlations, etc., which will be probed much better in the future. The  $s \leftrightarrow d$  processes, with lower SM rates, will provide many other challenging measurements and opportunities to find NP. Rare *B* decays can also be used as probes for “hidden sector” particle searches, for lepton flavor violation, and for baryon number violating processes.

There are also some intriguing deviations from the SM in the current data. The D0 collaboration measured the CP-violating dilepton asymmetry to be  $4\sigma$  away from zero,  $A_{\text{SL}}^b = (7.87 \pm 1.96) \times 10^{-3} \approx 0.6 A_{\text{SL}}^d + 0.4 A_{\text{SL}}^s$  [50]. The measured semileptonic asymmetry is a mixture of  $B_d$  and  $B_s$  ones, where  $A_{\text{SL}} \simeq 2(1 - |q/p|)$  in each case measures the mismatch of the CP and mass eigenstates. The quantity  $(1 - |q/p|)$  is model-

independently suppressed by  $m_b^2/m_W^2$ , with an additional  $m_c^2/m_b^2$  suppression in the SM, which NP may violate [51]. Since the D0 result allows plenty of room for NP, it will be important for LHCb and Belle II to clarify the situation. LHCb has recently measured  $A_{\text{SL}}^s = (-2.4 \pm 5.4 \pm 3.3) \times 10^{-3}$  [52] which complements  $A_{\text{SL}}^d$  measured at  $e^+e^- B$  factories. Further improvement in experimental errors on both quantities is needed.

Another interesting anomaly is the hint of the flavor universality violation in  $B \rightarrow D^{(*)}\tau\nu$  decays observed by BABAR [53] which differ from the SM prediction expected from the  $B \rightarrow D^{(*)}\ell\nu$  rates by  $3.4\sigma$ . Combined with the slight excess of  $\mathcal{B}(B \rightarrow \tau\nu)$  over the SM the measurements can be explained using charged Higgs exchange, e.g., in the two Higgs doublet model, but with nontrivial flavor structure [54]. The MFV hypothesis is not preferred. To settle the case it will require larger data sets at the future  $e^+e^- B$  factories (and measuring the  $B \rightarrow \mu\bar{\nu}$  mode as well).

Any of the above measurements could lead to a discovery of new physics. In addition, a real strength of the  $B$  physics program is that a pattern of modifications in different measurements can help to zoom in on the correct NP model. Further information will also be provided by rare kaon decay experiments and searches for lepton flavor violation in charged lepton decays such as  $\mu \rightarrow e\gamma$ ,  $\mu$ -to- $e$  conversion on a nucleus,  $\tau \rightarrow \mu\gamma$ , and  $\tau \rightarrow 3\mu$ . This program will provide complementary information to the on-shell searches at the LHC.

### Bottomonium Spectroscopy

Recent observations of the spin-singlet states  $h_b(1P)$ ,  $h_b(2P)$ , and  $\eta_b(2S)$  have contributed greatly to our understanding of bottomonium multiplets below the open-bottom threshold. The unexpected discovery of narrow, manifestly exotic  $b\bar{b}$  mesons above the open-bottom threshold has revealed a gap in our understanding of the QCD spectrum. Future data will probably reveal additional  $b\bar{b}$  threshold states. Understanding the spectrum and decays of these states are major challenges for lattice QCD and phenomenology. Comparisons of these bottomonium states with the  $XYZ$  states in the charmonium system should provide additional clues. The challenge of bottomonium spectroscopy is discussed in detail in a Snowmass White Paper [55].

## 4.2 Physics Potential of $e^+e^-$ Experiments: Belle II

The spectacular successes of the  $B$ -factory experiments Belle and BABAR highlight the advantages of  $e^+e^-$  collider experiments:

- Running on the  $\Upsilon(4S)$  resonance produces an especially clean sample of  $B^0\bar{B}^0$  pairs in a quantum correlated  $1^{--}$  state. The low background level allows reconstruction of final states containing  $\gamma$ 's and particles decaying to  $\gamma$ 's:  $\pi^0$ ,  $\rho^\pm$ ,  $\eta$ ,  $\eta'$ , etc. Neutral  $K_L^0$  mesons are also efficiently reconstructed. Detection of the decay products of one  $B$  allows the flavor of the other  $B$  to be tagged.
- Due to low track multiplicities and detector occupancy, the reconstruction efficiency is high and the trigger bias is low. This substantially reduces corrections and systematic uncertainties in many types of measurements, e.g., Dalitz plot analyses.
- By utilizing asymmetric beam energies, the Lorentz boost  $\beta$  of the  $e^+e^-$  system can be made large enough such that a  $B$  or  $D$  meson travels an appreciable distance before decaying. This allows precision measurements of lifetimes, mixing parameters, and CP violation (CPV). Note that measurement of the  $D$  lifetime provides a measurement of the mixing parameter  $y_{CP}$ , while measurement of the  $B$  lifetime (which is already well measured) allows one to determine the decay time resolution function from data.

- Since the absolute delivered luminosity is measured with Bhabha scattering, an  $e^+e^-$  experiment measures *absolute* branching fractions. These are complementary to *relative* branching fractions measured at hadron colliders, and in fact are used to normalize the relative measurements.
- Since the initial state is completely known, one can perform “missing mass” analyses, i.e., infer the existence of new particles via energy/momentum conservation rather than reconstructing their final states. By fully reconstructing a  $B$  decay in one hemisphere of the detector, inclusive decays such as  $B \rightarrow X_s \ell^+ \ell^-$ ,  $X_s \gamma$  can be measured in the opposite hemisphere.
- In addition to producing large samples of  $B$  and  $D$  decays, an  $e^+e^-$  machine produces large sample of  $\tau$  leptons. This allows one to measure rare  $\tau$  decays and search for forbidden  $\tau$  decays with a high level of background rejection.

To extend this physics program beyond the Belle and *BABAR* experiments, the KEKB  $e^+e^-$  accelerator at the KEK laboratory in Japan will be upgraded to SuperKEKB, and the Belle experiment will be upgraded to Belle II. The KEKB accelerator achieved a peak luminosity of  $2.1 \times 10^{34} \text{ cm}^{-2}\text{s}^{-1}$ , and the Belle experiment recorded a total integrated luminosity of  $1040 \text{ fb}^{-1}$  (just over  $1.0 \text{ ab}^{-1}$ ). The SuperKEKB accelerator plans to achieve a luminosity of  $8 \times 10^{35} \text{ cm}^{-2}\text{s}^{-1}$ , and the Belle II experiment plans to record  $50 \text{ ab}^{-1}$  of data by 2022. As  $\sigma(e^+e^- \rightarrow b\bar{b}) \approx 1.1 \text{ nb}$  at the  $\Upsilon(4S)$  resonance, this data sample will contain  $5 \times 10^{10} B\bar{B}$  pairs. Such a large sample will improve the precision of time-dependent CPV measurements and the sensitivity of searches for rare and forbidden decays. Systematic errors should also be reduced, as control samples from which many are calculated will substantially increase.

A discussion of the complete physics program of Belle II is beyond the scope of this summary. Here we touch upon only a few highlights. More complete writeups can be found in Refs. [56] and [57]; the latter was written in the context of the proposed — but declined — SuperB experiment in Italy. The expected sensitivity of Belle II in  $50 \text{ fb}^{-1}$  of data for various topical  $B$  decays is listed in Table 3.

As mentioned above, a main strength of a  $B$  factory experiment is the ability to make precision measurements of CP violation, and this capability will be exploited to search for NP sources of CPV. The difference between  $B^0$  and  $\bar{B}^0$  decay rates to a common self-conjugate state is sensitive to both direct CPV (i.e., occurring in the  $B^0$  and  $\bar{B}^0$  decay amplitudes), and indirect CPV from interference between the  $B \rightarrow f$  decay and  $B \rightarrow \bar{B}^0 \rightarrow f$  mixing amplitudes. The indirect CPV was originally measured at Belle and *BABAR* for all-charged final states such as  $J/\psi K^0$  [58, 59] (see Fig. 4, left) and  $\pi^+\pi^-$  [60, 61]; at Belle II, this measurement will be extended with good statistics to more challenging final states such as  $B^0 \rightarrow K_S^0 K_S^0$  (Fig. 4, left, shows a first measurement by Belle),  $B^0 \rightarrow K^0 \pi^0$ , and  $B^0 \rightarrow X_{s+d} \gamma$ . The last mode proceeds via electromagnetic  $b \rightarrow s\gamma$  and  $b \rightarrow d\gamma$  penguin amplitudes, where  $X_{s+d}$  represents the hadronic system in these decays. In a fully inclusive measurement, the  $\gamma$  is measured but  $X_{s+d}$  is not reconstructed. In the SM there is a robust expectation that direct CP violation is negligible, i.e., the decay rates for  $B$  and  $\bar{B}$  to  $X_{s+d} \gamma$  are equal. A measured difference would be a strong indication of NP, and differences of up to 10% appear in some non-SM scenarios. The best measurement with existing  $B$ -factory data is consistent with no difference and has a 7% absolute error [62]. Belle II should reduce this uncertainty to below 1%.

Both Belle and *BABAR* used the  $b \rightarrow c\bar{c}s$  “tree” mode  $B^0 \rightarrow J/\psi K^0$  to measure the phase  $\beta$  of the CKM unitary triangle to high precision:  $\sin(2\beta) = 0.665 \pm 0.022$  [63]. However, this phase can also be measured in  $b \rightarrow s\bar{s}s$  “loop” decays such as  $B^0 \rightarrow \phi K^0$  and  $B^0 \rightarrow \eta' K^0$ . Since virtual NP contributions could compete with the SM loop diagrams, these modes are sensitive to NP. Comparing the values of  $\sin(2\beta)$  measured in  $b \rightarrow c\bar{c}s$  and in  $b \rightarrow s\bar{s}s$  processes thus provides a way to search for NP. The decay  $B^0 \rightarrow \eta' K^0$  is the most precisely measured  $b \rightarrow s\bar{s}s$  mode; the value of  $\sin(2\beta)$  obtained is  $0.59 \pm 0.07$  [63], about  $1.2\sigma$  lower than that measured in  $B^0 \rightarrow J/\psi K^0$  decays. Belle II is expected to reduce this error by almost an order of magnitude, making the test much more sensitive.

Observable	SM theory	Current measurement (early 2013)	Belle II (50 ab <sup>-1</sup> )
$S(B \rightarrow \phi K^0)$	0.68	$0.56 \pm 0.17$	$\pm 0.03$
$S(B \rightarrow \eta' K^0)$	0.68	$0.59 \pm 0.07$	$\pm 0.02$
$\alpha$ from $B \rightarrow \pi\pi, \rho\rho$		$\pm 5.4^\circ$	$\pm 1.5^\circ$
$\gamma$ from $B \rightarrow DK$		$\pm 11^\circ$	$\pm 1.5^\circ$
$S(B \rightarrow K_S \pi^0 \gamma)$	$< 0.05$	$-0.15 \pm 0.20$	$\pm 0.03$
$S(B \rightarrow \rho \gamma)$	$< 0.05$	$-0.83 \pm 0.65$	$\pm 0.15$
$A_{\text{CP}}(B \rightarrow X_{s+d} \gamma)$	$< 0.005$	$0.06 \pm 0.06$	$\pm 0.02$
$A_{\text{SL}}^d$	$-5 \times 10^{-4}$	$-0.0049 \pm 0.0038$	$\pm 0.001$
$\mathcal{B}(B \rightarrow \tau \nu)$	$1.1 \times 10^{-4}$	$(1.64 \pm 0.34) \times 10^{-4}$	$\pm 0.05 \times 10^{-4}$
$\mathcal{B}(B \rightarrow \mu \nu)$	$4.7 \times 10^{-7}$	$< 1.0 \times 10^{-6}$	$\pm 0.2 \times 10^{-7}$
$\mathcal{B}(B \rightarrow X_s \gamma)$	$3.15 \times 10^{-4}$	$(3.55 \pm 0.26) \times 10^{-4}$	$\pm 0.13 \times 10^{-4}$
$\mathcal{B}(B \rightarrow K \nu \bar{\nu})$	$3.6 \times 10^{-6}$	$< 1.3 \times 10^{-5}$	$\pm 1.0 \times 10^{-6}$
$\mathcal{B}(B \rightarrow X_s \ell^+ \ell^-)$ ( $1 < q^2 < 6 \text{ GeV}^2$ )	$1.6 \times 10^{-6}$	$(4.5 \pm 1.0) \times 10^{-6}$	$\pm 0.10 \times 10^{-6}$
$A_{\text{FB}}(B^0 \rightarrow K^{*0} \ell^+ \ell^-)$ zero crossing	7%	18%	5%
$ V_{ub} $ from $B \rightarrow \pi \ell^+ \nu$ ( $q^2 > 16 \text{ GeV}^2$ )	9% $\rightarrow$ 2%	11%	2.1%

**Table 3.** The expected reach of Belle II with 50 ab<sup>-1</sup> of data for various topical  $B$  decay measurements. Also listed are the SM expectations and the current experimental results. For  $\mathcal{B}(B \rightarrow X_s \ell^+ \ell^-)$ , the quoted measurement [62] covers the full  $q^2$  range. For  $|V_{ub}|$  and the  $A_{\text{FB}}$  zero crossing, we list the fractional errors.

The  $B^0 \rightarrow K^0 \pi^0$  CP asymmetry is an important component of a sum rule which holds in the isospin limit [64]

$$\mathcal{A}_{K^+ \pi^-} \frac{\mathcal{B}_{K^+ \pi^-}}{\tau_{B^0}} + \mathcal{A}_{K^0 \pi^+} \frac{\mathcal{B}_{K^0 \pi^+}}{\tau_{B^+}} = 2\mathcal{A}_{K^+ \pi^0} \frac{\mathcal{B}_{K^+ \pi^0}}{\tau_{B^+}} + 2\mathcal{A}_{K^0 \pi^0} \frac{\mathcal{B}_{K^0 \pi^0}}{\tau_{B^0}}, \quad (5)$$

where  $\mathcal{A}$  denotes a CP asymmetry,  $\mathcal{B}$  a branching fraction, and  $\tau$  a lifetime. This sum rule is thought to be accurate to a few percent precision and provides a robust test of the SM. The limitation of the test is the precision of  $\mathcal{A}_{K^0 \pi^0}$ , which is difficult to measure and currently known to only  $\sim 14\%$  precision [65]. At Belle II this is expected to be reduced to  $\sim 3\%$  precision, greatly improving the sensitivity of Eq. (5) to NP.

Numerous rare  $B$  decays that were observed with low statistics by Belle and BABAR or not at all will become accessible at Belle II. One example is  $B^+ \rightarrow \tau^+ \nu$ , which in the SM results from a  $W$ -exchange diagram and has an expected branching fraction of  $(0.76_{-0.06}^{+0.10}) \times 10^{-4}$  [66]. This mode is sensitive to supersymmetric models and others that predict the existence of a charged Higgs. The final state contains multiple neutrinos and thus is feasible to study only at an  $e^+ e^-$  experiment. The current average branching fraction from Belle and BABAR is  $(1.15 \pm 0.23) \times 10^{-4}$  [67, 68, 69, 70], somewhat higher than the SM expectation. Belle II should reduce this error to about  $0.04 \times 10^{-4}$ . The contribution of a charged Higgs boson within the context of a Type II Higgs doublet model (e.g., which is also the tree level Higgs sector of the Minimal Supersymmetric Model) would increase the branching fraction above the SM prediction by a factor  $1 - (m_B^2/m_H^2) \tan^2 \beta$ , where  $m_H$  is the mass of the charged Higgs and  $\tan \beta$  is the ratio of vacuum expectation values of up-type and down-type Higgses. This relation can be used in conjunction with the measured value of the branching fraction to constrain  $m_H$  and  $\tan \beta$ . The expected constraint from a  $B$ -factory experiment with 75 ab<sup>-1</sup> of data is shown in Fig. 4 (right). One sees that a large region of phase space is excluded. For  $\tan \beta \gtrsim 60$ , the range  $m_H < 2 \text{ TeV}/c^2$  is excluded.

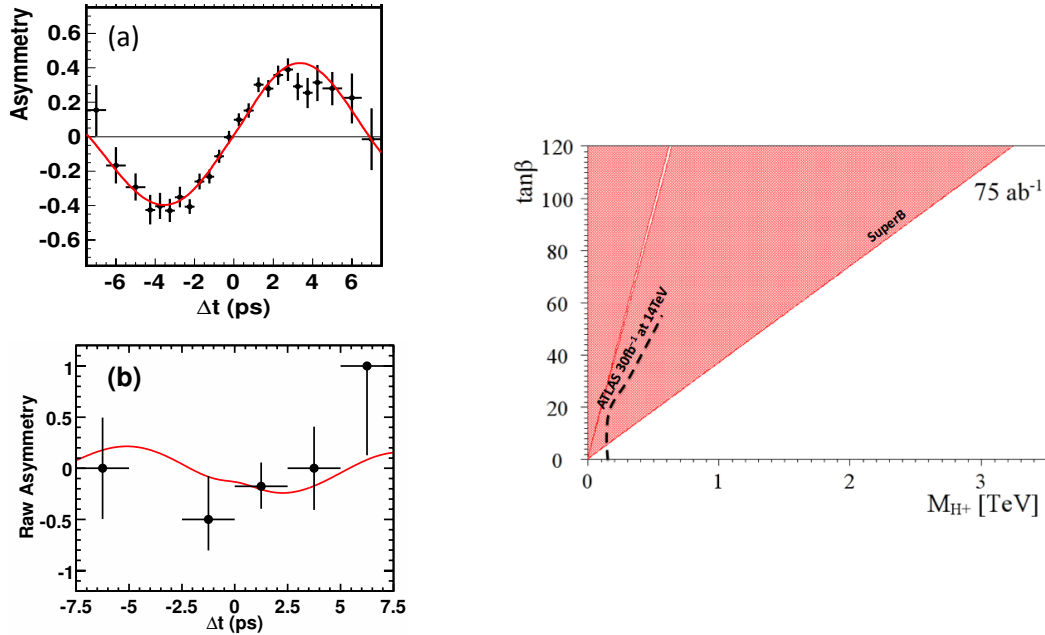


**Figure 4.** Left: Belle measurements of the time-dependent CP asymmetry versus  $\Delta t$  for (a)  $B \rightarrow J/\psi K^0$  and (b)  $B \rightarrow K_S^0 K_S^0$ . The parameter  $\sin(2\beta)$  is determined from the amplitude of the oscillations. Belle II should obtain statistics for  $B \rightarrow K_S^0 K_S^0$  (and other loop-dominated modes) comparable to those obtained by Belle for  $B \rightarrow J/\psi K^0$ . Right: The expected constraint in  $m_H$  vs.  $\tan\beta$  parameter space for a Type II Higgs doublet model that would result from 75  $\text{ab}^{-1}$  of data at a super-B-factory. For comparison, also shown is the expected constraint from ATLAS in 30  $\text{fb}^{-1}$  of data.

Other interesting processes include  $b \rightarrow s\ell^+\ell^-$  and  $b \rightarrow d\ell^+\ell^-$ , with  $\ell = e$  or  $\mu$ . These are also sensitive to NP via loop diagrams. Belle II will reconstruct a broad range of exclusive final states such as  $B \rightarrow K^{(*)}\ell^+\ell^-$ , from which one can determine CP asymmetries, forward-backward asymmetries, and isospin asymmetries (i.e., the asymmetry between  $B^+ \rightarrow K^{(*)+}\ell^+\ell^-$  and  $B^0 \rightarrow K^{(*)0}\ell^+\ell^-$ ). Belle II will also measure inclusive processes such as  $B \rightarrow X_{s+d}\ell^+\ell^-$ , for which theoretical predictions have less uncertainty than those for exclusive processes. By running on the  $\Upsilon(5S)$  resonance, Belle II can study  $B_s^0$  decays. Topical decay modes include  $B_s^0 \rightarrow D_s^{*+}D_s^{*-}$ ,  $D_s^{*+}\rho^-$ , and  $B_s^0 \rightarrow \gamma\gamma$ , all of which are challenging in a hadronic environment.

The SuperKEKB project at KEK is well underway. Commissioning of the accelerator is expected to begin in 2015. The high luminosity ( $8 \times 10^{35} \text{ cm}^{-2}\text{s}^{-1}$ , 40 times larger than KEKB) results mainly from a smaller  $\beta^*$  function and reduced emittance. As a result, the vertical beam spread at the interaction point will shrink from  $\sim 2 \mu\text{m}$  at KEKB to  $\sim 60 \text{ nm}$  at SuperKEKB. In addition, the beam currents will be approximately doubled, and the beam-beam parameter will be increased by 50%.

The Belle II detector will be an upgraded version of the Belle detector that can handle the increased backgrounds associated with higher luminosity. The inner vertex detector will employ DEPLETED Field Effect (DEPFET) pixels located inside a new silicon strip tracker employing the APV25 ASIC (developed for CMS) to handle the large rates. There will also be a new small-cell drift chamber. The particle identification system will consist of an “imaging-time-of-propagation” (iTOP) detector in the barrel region, and an aerogel-radiator-based ring-imaging Cherenkov detector in the forward endcap region. The iTOP operates in a similar manner as BABAR’s DIRC detector, except that the photons are focused with a spherical mirror onto a finely segmented array of multi-channel-plate (MCP) PMTs. These MCP PMTs provide precise timing, which significantly improves the discrimination power between pions and kaons over that provided by imaging

alone. The CsI(Tl) calorimeter will be retained but instrumented with waveform sampling readout. The innermost layers of the barrel  $K_L^0/\mu$  detector, and all layers of the endcap  $K_L^0/\mu$  detector, will be upgraded to use scintillator in order to accommodate the higher rates. Belle II should be ready to roll in by the spring of 2016 after commissioning of SuperKEKB is completed. The U.S. groups on Belle II are focusing their efforts on the iTOP and  $K_L^0/\mu$  systems.

### 4.3 Physics Potential of Hadronic Experiments

#### LHCb and its Upgrade

The spectacular successes of LHCb have realized some of the great potential for studying the decays of particles containing  $c$  and  $b$  quarks at hadron colliders. The production cross sections are quite large. More than 100 kHz of  $b$ -hadrons within the detector acceptance can be produced even at reduced LHC luminosities ( $4 \times 10^{32} \text{ cm}^{-2}\text{s}^{-1}$ ). This is a much higher production rate than can be achieved even in the next generation  $e^+e^- B$  factories. All species of  $b$ -flavored hadrons, including  $B_s$  and  $B_c$  mesons, and  $b$  baryons, are produced. However, compared to  $e^+e^-$  colliders, the environment is much more harsh for experiments. At hadron colliders, the  $b$  quarks are accompanied by a very high rate of background events; they are produced over a very large range of momenta and angles; and even in  $b$ -events of interest there is a complicated underlying event. The overall energy of the center of mass of the hard scatter that produces the  $b$  quark, which is usually from the collision of a gluon from each beam particle, is not known, so the overall energy constraint that is so useful in  $e^+e^-$  colliders is not available. These features translate into challenges in triggering, flavor tagging, and photon detection and they limit the overall efficiency.

The CDF and D0 experiments at the Fermilab Tevatron demonstrated that these problems could be successfully addressed using precision silicon vertex detectors and specialized triggers. While these experiments were mainly designed for high- $p_T$  physics, they made major contributions to bottom and charm physics [71, 72].

The LHC produced its first collisions at 7 TeV center of mass energy at the end of March 2010. The  $b$  cross section at the LHC is  $\sim 300 \mu\text{b}$ , a factor of three higher than at the Tevatron and approximately 0.5% of the inelastic cross section. When the LHC reaches its design center of mass energy of 14 TeV in 2015, the cross section will be a factor of two higher.

The LHC program features for the first time at a hadron collider a dedicated  $B$ -physics experiment, LHCb [73]. LHCb covers the forward direction from about 10 mr to 300 mr with respect to the beam line.  $B$  hadrons in the forward direction are produced by collisions of gluons of unequal energy, so that the center of mass of the collision is Lorentz boosted in the direction of the detector. Because of this, the  $b$ -hadrons and their decay products are produced at small angles with respect to the beam and have momenta ranging from a few GeV/ $c$  to more than a hundred GeV/ $c$ . Because of the Lorentz boost, even though the angular range of LHCb is small, its coverage in pseudorapidity is between about 2 – 5, and both  $b$  hadrons travel in the same direction, making  $b$  flavor tagging possible. With the small angular coverage, LHCb can stretch out over a long distance along the beam without becoming too large transversely. A silicon microstrip vertex detector (VELO) only 8 mm from the beam provides precision tracking that enables LHCb to separate weakly decaying particles from particles produced at the interaction vertex. This allows the measurement of lifetimes and oscillations due to flavor mixing. A 4 Tm dipole magnet downstream of the collision region, in combination with the VELO, large area silicon strips (TT) placed downstream of the VELO but upstream of the dipole, and a combination of silicon strips (IT) and straw tube chambers (OT) downstream of the dipole provides a magnetic spectrometer with excellent mass resolution. There are two ring imaging Cherenkov (RICH) counters, one upstream of the dipole and one downstream, that together

provide  $K-\pi$  separation from 2 to 100 GeV/ $c$ . An electromagnetic calorimeter (ECAL) follows the tracking system and provides electron triggering and  $\pi^0$  and  $\gamma$  reconstruction. This is followed by a hadron calorimeter (HCAL) for triggering on hadronic final states. A muon detector at the end of the system provides muon triggering and identification.

LHCb has a very sophisticated trigger system [74] that uses hardware at the lowest level (L0) to process the signals from the ECAL, HCAL and muon systems. The L0 trigger reduces the rate to  $\sim 1$  MHz followed by the High Level Trigger (HLT), a large computer cluster, that reduces the rate to  $\sim 3$  kHz for archiving to tape for physics analysis. LHCb is able to run at a luminosity of  $4.0 \times 10^{32} \text{ cm}^{-2}\text{s}^{-1}$ . This is much smaller than the current peak luminosity achieved by the LHC and only a few percent of the LHC design luminosity. The luminosity that LHCb can take efficiently is currently limited by the 1 MHz bandwidth between the Level 0 trigger system and the trigger cluster. Therefore, the physics reach of LHCb is determined by the detector capabilities and not by the machine luminosity. In fact, LHC implemented a “luminosity leveling” scheme in the LHCb collision region so that LHCb could run at its desired luminosity throughout the store while the other experiments, CMS and ATLAS, could run at higher luminosities. This mode of running will continue until 2017 when a major upgrade [75, 76] of the LHCb trigger and parts of the detector and front end electronics will increase the bandwidth to the HLT, increase archiving rate to 20 kHz, and permit operation at a factor of 10 higher luminosity. Several subdetectors will be rebuilt for more robust performance at higher luminosities, including VELO (pixels), TT (finer strips), IT+OT (technology to be soon decided) and RICH (redesigned optics, MaPMTs).

There have been three runs of the LHC. In the first “pilot” run in 2010, LHCb recorded  $35 \text{ pb}^{-1}$ , which was enough to allow it to surpass in precision many existing measurements of  $B$  decays. In 2011, the LHC delivered more than  $5 \text{ fb}^{-1}$  to CMS and ATLAS. Since this luminosity was more than LHCb was designed to handle, the experiment ran at a maximum luminosity that was 10% of the LHC peak luminosity. The total integrated luminosity was about  $1 \text{ fb}^{-1}$ . In 2012 LHC delivered  $20 \text{ fb}^{-1}$  to CMS and ATLAS with additional  $2 \text{ fb}^{-1}$  collected by LHCb. Until the LHCb upgrade is installed in the long shutdown planned in 2018, LHCb plans to run at a luminosity of  $4.0 \times 10^{32} \text{ cm}^{-2}\text{s}^{-1}$ . Between now and then, LHCb will accumulate about  $1\text{--}2 \text{ fb}^{-1}$  per operating year, so a total of about  $6.5 \text{ fb}^{-1}$  will be obtained. The sensitivity will increase by more than this because the LHC will run at 14 TeV, with about a factor of two higher  $B$  cross section. After the upgrade is installed, LHCb will integrate about  $5 \text{ fb}^{-1}$  per year, so that about  $50 \text{ fb}^{-1}$  will be obtained over the decade following the upgrade installation.

The decay  $B_s \rightarrow J/\psi\phi$  has been used to measure the CKM angle  $\phi_s (\equiv -2\beta_s)$  [44]. The result, using also the decay mode  $B_s \rightarrow J/\psi f_0$  [77] first established by LHCb [78], is  $\phi_s = 0.01 \pm 0.07 \pm 0.01 \text{ rad}$  [44]. The difference in the width of the CP-even and CP-odd  $B_s$  mesons is  $\Delta\Gamma_s = (0.106 \pm 0.011 \pm 0.007) \text{ ps}^{-1}$ . These results are consistent with the SM, resolving a slight tension with earlier measurements from the Tevatron, which deviated somewhat from the SM predictions. However, the experimental uncertainty on  $\phi_s$  is still a factor of 40 larger than that on the SM prediction, so improved measurements will probe higher mass scales of possible NP contributions.

The rare decay  $B_s \rightarrow \mu^+\mu^-$  is predicted in the SM to have a branching fraction  $(3.54 \pm 0.30) \times 10^{-9}$  [46, 47]. A higher or lower branching fraction would be an indicator for NP. LHCb presented first evidence of this decay based on  $2.1 \text{ fb}^{-1}$  of data, with  $\mathcal{B}(B_s \rightarrow \mu^+\mu^-) = (3.2^{+1.5}_{-1.2}) \times 10^{-9}$  [45] consistent with the SM prediction. LHCb has recently updated its result for  $3 \text{ fb}^{-1}$  of data to  $\mathcal{B}(B_s \rightarrow \mu^+\mu^-) = (2.9^{+1.1}_{-1.0}) \times 10^{-9}$  [49]. (CMS has also recently reported a measurement of  $\mathcal{B}(B_s \rightarrow \mu^+\mu^-) = (3.0^{+1.0}_{-0.9}) \times 10^{-9}$  [48].) LHCb has also set an upper limit on  $\mathcal{B}(B_d \rightarrow \mu^+\mu^-) < 0.74 \times 10^{-9}$  (95% C.L.) with the  $3 \text{ fb}^{-1}$  data set. These measurements impose stringent constraints on SUSY models as illustrated in Fig. 5. Further increase in statistics will probe even higher energy scales.

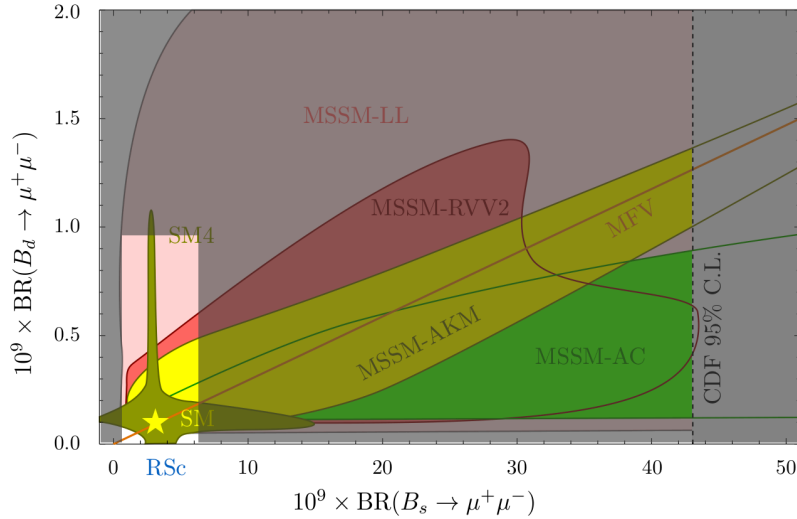


**Figure 5.** Correlation between the branching ratios of  $B_s^0 \rightarrow \mu^+\mu^-$  and  $B_d^0 \rightarrow \mu^+\mu^-$  in various models. The SM point is marked by a star. From Ref. [81] with the  $2.1 \text{ fb}^{-1}$  correction LHCb result [45] superimposed.

LHCb has also produced results on the key decay  $B^0 \rightarrow K^{*0}\mu^+\mu^-$  ( $1.1 \text{ fb}^{-1}$ ) [82] that could reveal evidence for NP. One of the interesting observables is the forward-backward asymmetry of the  $\mu^-$  relative to the direction of the parent  $B^0$  meson in the dimuon center of mass vs.  $q^2$  (dimuon invariant mass). The SM prediction crosses zero within a well-determined narrow region of  $q^2$ , due to the interference between the SM box and electroweak penguin diagrams. NP can remove the crossover or displace its location. Indications from low statistics at Belle, BABAR, and CDF seemed to indicate that this might be happening. The LHCb results are the most precise so far, and are in good agreement with the SM within errors, which however can be significantly reduced with the LHCb upgrade. Many other observables sensitive to NP have also been investigated. The CMS ( $5.2 \text{ fb}^{-1}$  [83]) and ATLAS ( $4.9 \text{ fb}^{-1}$  [84]) Collaborations have also performed such studies. The results agree with the SM and the previous measurements, but have larger errors than LHCb.

Many other decays are being studied, including all-hadronic decays such as  $B_s \rightarrow \phi\phi$  [85] ( $\beta_s^{\text{eff}}$  via interference of mixing and decay via gluonic penguin)  $B \rightarrow D\pi$ ,  $B \rightarrow DK$  (determination of  $\gamma$  from tree processes), and states with photons such as  $B_s \rightarrow \phi\gamma$  (search for right-handed currents). The expected sensitivity to selected important  $B$  decays during the present and upgraded phases of the LHCb experiment is shown in Table 4. In addition, LHCb has also demonstrated the capability for a rich program of studies of  $B_c$  meson decays.

The physics output of LHCb also extends beyond its  $B$  and charm (see next section) core programs. Examples of other topics include measurements of the production of electroweak gauge bosons in the forward kinematic region covered by the LHCb acceptance [86], studies of double parton scattering [87], measurements of the properties of exotic hadrons [88, 89], searches for lepton number and lepton flavor violations [90, 91] and for long-lived new particles [92].

## ATLAS and CMS

Two LHC detectors, CMS and ATLAS, are designed to explore high mass and high- $p_T$  phenomena to look for new physics at the LHC. They must operate at luminosities of up to  $10^{34} \text{ cm}^{-2}\text{s}^{-1}$ , which implies the need to handle an average event pileup of  $\sim 20$ . Both experiments can implement muon triggers with relatively low thresholds of a few  $\text{GeV}/c$ . However, the rate of low- $p_T$  muons from  $B$  decays competes for scarce resources



Observable	Current SM theory uncertainty	Precision as of 2013	LHCb (6.5 fb <sup>-1</sup> )	LHCb Upgrade (50 fb <sup>-1</sup> )
$2\beta_s(B_s \rightarrow J/\psi\phi)$	$\sim 0.003$	0.09	0.025	0.008
$\gamma(B \rightarrow D^{(*)}K^{(*)})$	$< 1^\circ$	8°	4°	0.9°
$\gamma(B_s \rightarrow D_s K)$	$< 1^\circ$	—	$\sim 11^\circ$	2°
$\beta(B^0 \rightarrow J/\psi K_S^0)$	small	0.8°	0.6°	0.2°
$2\beta_s^{\text{eff}}(B_s \rightarrow \phi\phi)$	0.02	1.6	0.17	0.03
$2\beta_s^{\text{eff}}(B_s \rightarrow K^{*0}\bar{K}^{*0})$	$< 0.02$	—	0.13	0.02
$2\beta_s^{\text{eff}}(B_s \rightarrow \phi\gamma)$	0.2%	—	0.09	0.02
$2\beta^{\text{eff}}(B^0 \rightarrow \phi K_S^0)$	0.02	0.17	0.30	0.05
$A_{\text{SL}}^s$	$0.03 \times 10^{-3}$	$6 \times 10^{-3}$	$1 \times 10^{-3}$	$0.25 \times 10^{-3}$
$\mathcal{B}(B_s \rightarrow \mu^+\mu^-)$	8%	36%	15%	5%
$\mathcal{B}(B^0 \rightarrow \mu^+\mu^-)/\mathcal{B}(B_s \rightarrow \mu^+\mu^-)$	5%	—	$\sim 100\%$	$\sim 35\%$
$A_{\text{FB}}(B^0 \rightarrow K^{*0}\mu^+\mu^-)$ zero crossing	7%	18%	6%	2%

**Table 4.** Sensitivity of LHCb to key observables. The current sensitivity (based on 1–3 fb<sup>-1</sup>, depending on the measurement) is compared to that expected after 6.5 fb<sup>-1</sup> and that achievable with 50 fb<sup>-1</sup> by the upgraded experiment assuming  $\sqrt{s} = 14$  TeV. Note that at the upgraded LHCb, the yield per fb<sup>-1</sup>, especially in hadronic  $B$  and  $D$  decays, will be higher on account of the software trigger. (Adapted from Ref. [75].)

with the many other trigger signatures that could contain direct evidence of new physics. Thus in practice, only  $B$  final states containing dimuons are well preserved through the trigger pipelines. The trigger efficiency is lower than in LHCb but at higher luminosity. One example of this, discussed above, is the rare decay  $B_{d,s} \rightarrow \mu^+\mu^-$ . CMS has very recently reported a measurement of  $\mathcal{B}(B_s \rightarrow \mu^+\mu^-) = (3.0_{-0.9}^{+1.0}) \times 10^{-9}$  [48]. If ATLAS and CMS can maintain their trigger efficiency as the LHC luminosity and energy increase, they can be competitive in this study. The decay  $B^0 \rightarrow K^*\mu^+\mu^-$  presents more problems. The muons are softer and more difficult to trigger on and the limited  $K$ - $\pi$  separation increases the background to the  $K^*$ . However, as illustrated by their preliminary results these two experiments can play a confirming role to LHCb in this study. Despite their limitations, these two experiments will collect large numbers of  $B$  decays and should be able to observe many new decay modes and new particles containing  $b$  and charm quarks.

## 5 Report of the Charm Task Force

### 5.1 Introduction to Charm Physics

Studies of charm quarks can be split into two broad categories. First, in indirect searches for new physics affecting decays and oscillations, charm quarks furnish a unique probe of flavor physics in the up-quark sector, complementing strange and bottom physics. Second, as a probe of quantum chromodynamics (QCD) charm aids our understanding of nonperturbative physics, since it is not much heavier than the characteristic scale  $\Lambda \sim 1$  GeV of QCD. Overall, charm adds much to the core new physics thrusts in heavy flavor physics while also adding significant breadth to the program.

Charm physics measurements allow for direct determination of the Cabibbo-Kobayashi-Maskawa (CKM) matrix elements  $|V_{cs}|$  and  $|V_{cd}|$ , can also help improve the accuracy of  $|V_{cb}|$  and  $|V_{ub}|$  determined from  $B$

decays, and  $|V_{ts}|$  and  $|V_{td}|$  from  $B^0$  and  $B_s^0$  mixing. Part of this richness is due to the usefulness of charm data in verifying lattice QCD (LQCD) results.

Indirect searches for new physics with charm quarks provide competitive as well as complementary constraints to the results of direct searches at the Energy Frontier. One can classify searches in three broad categories, according to their “standard model background.”

1. Searches in the processes that are allowed in the standard model.

New physics contributions may often be difficult to discern in this case, except in cases of sufficient theoretical precision (e.g., leptonic decays of  $D$  mesons,  $D_q \rightarrow \ell\bar{\nu}$ ). Alternatively, testing relations that are only valid in the standard model, but not in BSM models, may prove advantageous; e.g., CKM triangle relations.

2. Searches in the processes that are forbidden in the standard model at tree level.

Flavor-changing neutral current (FCNC) interactions occur in the standard model only through loops and are therefore suppressed. New physics contributions can enter both at tree-level and from one-loop corrections. Examples include  $D^0 - \bar{D}^0$  mixing, or inclusive and exclusive transitions mediated by  $c \rightarrow u\gamma$  or  $c \rightarrow u\bar{\ell}\ell$ .

Searches for CP violation in charm decays and oscillations should be included here as well, as they require at least two different pathways to reach the final state, at least one of which is FCNC transition.

3. Searches in the processes that are forbidden in the standard model.

While these processes are generally very rare even in NP models, their observation, however, would constitute a high-impact discovery. Examples include searches for lepton- and baryon-number-violating transitions, such as  $D^0 \rightarrow e^+\mu^-$ ,  $D^0 \rightarrow \bar{p}e^+$ , etc.

The QCD side of charm physics is also very vibrant. Recently, there has been much activity in XYZ state spectroscopy, in addition to continued studies of conventional charmonium. This provides a rich source of results in hadronic physics and radiative transitions.

## 5.2 Current and Future Experiments

Over the past decade, charm results have been dominated by results from detectors at the  $e^+e^-$  flavor factories: BaBar, Belle, and CLEO-c. Currently, the BESIII experiment is running at charm threshold and Belle II, which will run at and near the  $\Upsilon(4S)$ , is under construction; both experiments have excellent capabilities in charm [93, 56]. While charm statistics are lower at threshold, the data are unique in their ability to measure strong phases and also excel at modes with neutrinos in the final state. The Belle II detector should begin physics running in 2017; charm from continuum fragmentation at  $B$ -factory energies is complementary to threshold data.

Hadron machines also provide important results. CDF was able to contribute due to displaced-vertex and muon triggers, producing notable results on  $D^0 - \bar{D}^0$  oscillations. While muon triggers have produced some charm results from ATLAS and CMS, the current and future charm program at hadron colliders lies almost exclusively with the dedicated flavor experiment, LHCb. Many areas of charm physics are accessible at LHCb and the 2018 upgrade will enhance opportunities even more. Their physics reach [75, 94] is an important addition to the  $e^+e^-$  program.

The BESIII program should continue at least until the end of the decade, and Belle II and LHCb will carry charm physics well into the 2020's. One major decision point is the future of threshold charm after BESIII.

Currently, the Cabibbo Lab near Rome is preparing a threshold tau-charm factory proposal. Interest has also been expressed by BINP at Novosibirsk and institutions in Turkey.

Another source of information on charm could come from fixed target experiments, of which the only currently approved example is PANDA [95] at the FAIR facility at Darmstadt, which will collide antiprotons in a storage ring with gas, solid, or liquid targets. The ability of that experiment to contribute will depend on the cross section for charm production by low energy antiprotons, a quantity that has not been measured and whose theoretical estimates vary from  $1\mu\text{b}$  to  $10\mu\text{b}$ , and the amount of time dedicated to the charm program, which competes with other aspects of the program that require the machine to operate below or close to the bare charm production threshold.

### Leptonic and Semileptonic Decays and CKM triangle relations

In leptonic and semileptonic decays, all of the uncertainties from strong-interaction effects may be conveniently parametrized as decay constants and form factors, respectively. The remainder of the theory is straightforward weak-interaction physics. Indeed, comparing decay constants and form factors to LQCD predictions allows one to exclude large portions of parameter space for NP models with charged scalars.

Leptonic decay rates depend on the square of both decays constants and CKM matrix elements. If one uses LQCD as in input, then  $|V_{cq}|$  may be extracted. If the CKM matrix elements are taken from elsewhere (possibly unitarity constraints), then we can test LQCD results. In fact, by taking ratios of leptonic and semileptonic decays, one can cancel  $|V_{cq}|$  to obtain pure LQCD tests.

The Cabibbo-suppressed leptonic decay  $D^+ \rightarrow \mu\nu$  is only measurable at threshold charm machines. Currently, it is essentially determined via one CLEO-c result [96], although BESIII has a preliminary result based on a dataset 3.5 times larger [97]. This result,  $f_D = (203.91 \pm 5.72 \pm 1.91)$  MeV, based on  $2.9 \text{ fb}^{-1}$ , is still statistics-limited.

The Cabibbo-favored  $D_s^+ \rightarrow \mu\nu, \tau\nu$  process is easier in two respects. Unlike the  $D^+$  case, where  $\tau\nu$  is a relatively small effect, here it offers additional channels that enhance the utility of a dataset. In addition,  $B$  factories possess enough tagging power in continuum charm production to make the best current single measurement. The one drawback is that  $D_s$  production rates are smaller than  $D^+$ . Currently, the best measurement of  $f_{D_s}$  is a preliminary result from Belle [98].

Successful LQCD calculations of  $D_{(s)}$  decay constants will give confidence in their results for  $B$  decay constants. And while  $f_B$  can be obtained from  $B \rightarrow \tau\nu$ , there is no analogous direct way to determine  $f_{B_s}$ . By contrast, in charm, both strange and non-strange decay constants are directly accessible.

The key semileptonic modes are  $D^0 \rightarrow K^- e^+ \nu, \pi^- e^+ \nu$ . Additional statistical power may be obtained by including the isospin-related  $D^+$  decays, but both CKM matrix elements are accessible without the need for the more experimentally challenging  $D_s$  decays. The form factors,  $f_K(q^2)$  and  $f_\pi(q^2)$ , are useful tests of LQCD. One depends on similar LQCD calculations to extract  $|V_{ub}|$  from  $B \rightarrow \pi\ell\nu$  decays.

For leptonic charm decays,  $f_{D_{(s)}}$  parametrizes the probability that the heavy and light quarks “find each other” to annihilate. Due to helicity suppression the rate goes as  $m_\ell^2$ , and many NP models could have a different parametric dependence on  $m_\ell^2$ . New physics can be discussed in terms of generalized couplings [99]. Models probed by this decay include extended Higgs sectors, which contain new charged scalar states, or models with broken left-right symmetry, which include heavy vector  $W_R^\pm$  states.

One can also search for new physics by testing relations that hold in the SM, but not necessarily in general. An example of such relation is a CKM “charm unitarity triangle” relation:

$$V_{ud}^* V_{cd} + V_{us}^* V_{cs} + V_{ub}^* V_{cb} = 0. \quad (6)$$

Processes that are used to extract CKM parameters in Eq. (6) can be affected by new physics. This can lead to disagreement between CKM elements extracted from different processes, or the triangle not closing. Finally, since all CP-violating effects in the flavor sector of the SM are related to the single phase of the CKM matrix, all of the CKM unitarity triangles, have the same area,  $A = J/2$ , where  $J$  is the Jarlskog invariant. This fact could provide a non-trivial check of the standard model, given measurements of more than one triangle with sufficient accuracy. Unfortunately, the charm unitarity triangle will be harder to work with than the familiar  $B$  physics triangle since it is rather “squashed.” In terms of the Wolfenstein parameter  $\lambda = 0.22$ , the relation in Eq. (6) has one side  $\mathcal{O}(\lambda^5)$  with the other two being  $\mathcal{O}(\lambda)$ .

### $D^0$ Oscillations (including CP Violation)

The presence of  $\Delta C = 2$  operators produce off-diagonal terms in the  $D^0 - \bar{D}^0$  mass matrix, mixing the flavor eigenstates into the mass eigenstates

$$|D_{1,2}\rangle = p|D^0\rangle \pm q|\bar{D}^0\rangle. \quad (7)$$

Neglecting CP violation leads to  $|p| = |q| = 1/\sqrt{2}$ . The mass and width splittings between the mass eigenstates are

$$x = \frac{m_1 - m_2}{\Gamma_D}, \quad y = \frac{\Gamma_1 - \Gamma_2}{2\Gamma_D}, \quad (8)$$

where  $\Gamma_D$  is the average width of the two mass eigenstates.

The oscillation parameters  $x$  and  $y$  are both of order 1% in the  $D^0$  system. These small values require the high statistics of  $B$  factories and hadron machines. Observations thus far have relied on the time-dependence of several hadronic decays  $K\pi$ ,  $K\pi\pi^-$ ,  $K_S\pi\pi$ , etc., as well as lifetime differences between CP-eigenstate decays ( $KK$ ,  $\pi\pi$ ) and the average lifetime (see the review in [62]). LHCb has made the highest significance ( $9\sigma$ ) observation of  $D^0$  oscillations in a single experiment [100]. However, a non-zero value of  $x$  has not yet been established at  $3\sigma$ . LHCb and Belle II will be able to pinpoint the value of  $x$  in the next several years.

Theoretical predictions for  $x$  and  $y$  in the SM are uncertain, although values as high as 1% had been expected [101]. The predictions need to be improved, and several groups are working to understand the problem using technology such as the heavy-quark expansion, lattice QCD, and other long-distance methods.

However, one can place an upper bound on the NP parameters by neglecting the SM contribution altogether and assuming that NP saturates the experimental result. One subtlety is that the SM and NP contributions can have either the same or opposite signs. While the sign of the SM contribution cannot be calculated reliably due to hadronic uncertainties,  $x$  computed within a given NP model can be determined. This stems from the fact that NP contributions are generated by heavy degrees of freedom, making the short-distance calculation reliable.

Any NP degree of freedom will generally be associated with a generic heavy mass scale  $\Lambda$ , at which the NP interaction is most naturally described. At the scale  $m_c$ , this description must be modified by the effects of QCD. In order to see how NP might affect the mixing amplitude, it is instructive to consider off-diagonal terms in the neutral D mass matrix,

$$M_{12} - \frac{i}{2}\Gamma_{12} = \frac{1}{2M_D} \langle \bar{D}^0 | \mathcal{H}_w^{\Delta C=-2} | D^0 \rangle + \frac{1}{2M_D} \sum_n \frac{\langle \bar{D}^0 | \mathcal{H}_w^{\Delta C=-1} | n \rangle \langle n | \mathcal{H}_w^{\Delta C=-1} | D^0 \rangle}{M_D - E_n + i\epsilon}, \quad (9)$$

where the first term contains  $\mathcal{H}_w^{\Delta C=-2}$ , which is an effective  $|\Delta C| = 2$  Hamiltonian, represented by a set of operators that are local at the  $\mu \sim m_D$  scale. This first term only affects  $x$ , but not  $y$ .

As mentioned above, heavy BSM degrees of freedom cannot be produced in charm meson decays, but can nevertheless affect the effective  $|\Delta C| = 2$  Hamiltonian by changing Wilson coefficients and introducing new operator structures. By integrating out those new degrees of freedom associated with a high scale  $\Lambda$ , we are left with an effective Hamiltonian written in the form of a series of operators of increasing dimension. It turns out that a model-independent study of NP  $|\Delta C| = 2$  contributions is possible, as any NP model will only modify Wilson coefficients of those operators [102, 103],

$$\mathcal{H}_{\text{NP}}^{|\Delta C|=2} = \frac{1}{\Lambda^2} \sum_{i=1}^8 C_i(\mu) Q_i(\mu), \quad \begin{aligned} Q_1 &= (\bar{u}_L^\alpha \gamma_\mu c_L^\alpha) (\bar{u}_L^\beta \gamma^\mu c_L^\beta), & Q_5 &= (\bar{u}_R^\alpha c_L^\beta) (\bar{u}_L^\beta c_R^\alpha), \\ Q_2 &= (\bar{u}_R^\alpha c_L^\alpha) (\bar{u}_R^\beta c_L^\beta), & Q_6 &= (\bar{u}_R^\alpha \gamma_\mu c_R^\alpha) (\bar{u}_R^\beta \gamma^\mu c_R^\beta), \\ Q_3 &= (\bar{u}_R^\alpha c_L^\beta) (\bar{u}_R^\beta c_L^\alpha), & Q_7 &= (\bar{u}_L^\alpha c_R^\alpha) (\bar{u}_L^\beta c_R^\beta), \\ Q_4 &= (\bar{u}_R^\alpha c_L^\alpha) (\bar{u}_L^\beta c_R^\beta), & Q_8 &= (\bar{u}_L^\alpha c_R^\beta) (\bar{u}_L^\beta c_R^\alpha), \end{aligned} \quad (10)$$

where  $C_i$  are dimensionless Wilson coefficients, and the  $Q_i$  are the effective operators;  $\alpha$  and  $\beta$  are color indices. In total, there are eight possible operator structures contributing to  $|\Delta C| = 2$  transitions. Taking operator mixing into account, a set of constraints on the Wilson coefficients of Eq. (10) can be placed,

$$(|C_1|, |C_2|, |C_3|, |C_4|, |C_5|) \leq (57, 16, 58, 5.6, 16) \times 10^{-8} \left( \frac{\Lambda}{1 \text{ TeV}} \right)^2. \quad (11)$$

The constraints on  $C_6 - C_8$  are identical to those on  $C_1 - C_3$  [103]. Note that Eq. (11) implies that new physics particles have highly suppressed couplings to charm quarks. Alternatively, the tight constraints of Eq. (11) probe NP at the very high scales:  $\Lambda \geq (4 - 10) \times 10^3$  TeV for tree-level NP-mediated charm mixing and  $\Lambda \geq (1 - 3) \times 10^2$  TeV for loop-dominated mixing via new physics particles.

There is a beautiful effect at threshold, where the decay of the  $\psi(3770)$  gives a quantum correlated  $D^0 - \bar{D}^0$  pair, and like-sign  $K^\pm \pi^\mp$  decays at equal times only arise from mixing, without the doubly-Cabibbo-suppressed background. However, this requires high-quality particle identification, and is very luminosity-intensive. The event rate is of order one event per  $5 \text{ fb}^{-1}$  (the current BESIII dataset is  $2.9 \text{ fb}^{-1}$ ). Threshold does come into play in a different manner, however. When mixing is measured via the time dependence of hadronic decays, one measures  $x, y$  in a rotated basis. These parameters, denoted  $x', y'$  in the case of  $K^\pm \pi^\mp$ , can only be converted to the desired  $x, y$  with knowledge of a strong final-state scattering phase,  $\delta_{K\pi}$ . Threshold charm data provide the only possibility to measure this (and other related) phases.

CP violation in  $D^0 - \bar{D}^0$  mixing is an important area for future work. In Table 5, we summarize the prospects for future results on these topics. The entries related to  $q/p$  parametrize CP violation; in the absence of CP violation in mixing,  $|q/p| = 1$  and  $\arg(q/p) = 0$  in the phase convention adopted.

## CP Violation in Decays

A possible manifestation of new physics interactions in the charm system is associated with the observation of CP violation [104, 105]. This is due to the fact that all quarks that build up the hadronic states in weak decays of charm mesons belong to the first two generations. Since the  $2 \times 2$  Cabibbo quark mixing matrix is real, no CP violation is possible in the dominant tree-level diagrams which describe the decay amplitudes. CP-violating amplitudes can be introduced in the standard model by including penguin or box operators induced by virtual  $b$  quarks. However, their contributions are strongly suppressed by the small combination of CKM matrix elements  $V_{cb}V_{ub}^*$ . Thus, it was believed that the observation of large CP violation in charm

Observable	Current Expt.	LHCb (5 fb <sup>-1</sup> )	Belle II (50 ab <sup>-1</sup> )	LHCb Upgrade (50 fb <sup>-1</sup> )
$x$	$(0.63 \pm 0.20)\%$	$\pm 0.06\%$	$\pm 0.02\%$	$\pm 0.02\%$
$y$	$(0.75 \pm 0.12)\%$	$\pm 0.03\%$	$\pm 0.01\%$	$\pm 0.01\%$
$y_{\text{CP}}$	$(1.11 \pm 0.22)\%$	$\pm 0.02\%$	$\pm 0.03\%$	$\pm 0.01\%$
$ q/p $	$0.91 \pm 0.17$	$\pm 0.085$	$\pm 0.03$	$\pm 0.03$
$\arg(q/p)$	$(-10.2 \pm 9.2)^\circ$	$\pm 4.4^\circ$	$\pm 1.4^\circ$	$\pm 2.0^\circ$

**Table 5.** Sensitivities of Belle II and LHCb to charm mixing related parameters, along with the current results for these measurements; here  $\arg(q/p)$  means  $\arg[(q/p)(\bar{A}_{K^+K^-}/A_{K^+K^-})]$ . The second column gives the 2011 world averages. The remaining columns give the expected accuracy at the indicated integrated luminosities. In the convention used in HFAG fits, in the absence of CP violation  $|q/p| = 1$  and  $\arg(q/p) = 0$ .

decays or mixing would be an unambiguous sign for new physics. The SM “background” here is quite small, giving CP-violating asymmetries of the order of  $10^{-3}$ . Hence, observation of CP-violating asymmetries larger than 1% could indicate presence of new physics.

Recent measurements have indicated the possibility of direct CP violation in the decays  $D^0 \rightarrow K^+K^-$  and  $D^0 \rightarrow \pi^+\pi^-$  [106]. The current world average is

$$\Delta A_{\text{CP}} = A_{\text{CP}}(K^-K^+) - A_{\text{CP}}(\pi^-\pi^+) = -(0.33 \pm 0.12)\%, \quad (12)$$

although the most recent LHCb result (included in this average) has a central value with the opposite sign. These results triggered intense theoretical discussions of the possible size of this quantity in the standard model and in models of new physics [107]. New measurements of individual direct CP-violating asymmetries entering Eq. (12) and other asymmetries in the decays of neutral and charged  $D$ 's into  $PP$ ,  $PV$ , and  $VV$  final states are needed to guide theoretical calculations (of penguin amplitudes).

It is also important to measure CP-violating asymmetries in the decays of charmed baryon states, as those could have different theoretical and experimental systematics and could provide a better handle on theoretical uncertainties.

No indirect CP violation has been observed in charm transitions yet. However, available experimental constraints can provide some tests of CP-violating NP models. For example, a set of constraints on the imaginary parts of Wilson coefficients of Eq. (10) can be placed,

$$(|\text{Im}C_1|, |\text{Im}C_2|, |\text{Im}C_3|, |\text{Im}C_4|, |\text{Im}C_5|) < (11, 2.9, 11, 1.1, 3.0) \times 10^{-8} \left( \frac{\Lambda}{1 \text{ TeV}} \right)^2. \quad (13)$$

Just like the constraints of Eq. (11), they give a sense of how NP particles couple to the standard model.

## Rare Decays

The flavor-changing neutral current (FCNC) decay  $D^0 \rightarrow \mu^+\mu^-$  is of renewed interest after the measurement of  $B_s \rightarrow \mu^+\mu^-$ . While heavily GIM-suppressed, long-distance contributions from  $D^0 \rightarrow \gamma\gamma$ , for example, also contribute. Direct knowledge of the decay  $D^0 \rightarrow \gamma\gamma$  allows one to limit these contributions to the di-muon mode to below  $6 \times 10^{-11}$ .

Decays  $B \rightarrow K^{(*)}\ell^+\ell^-$  have been the subject of great interest for many years, both rates and angular distributions offer the chance to see new physics effects. The analogous charm decays,  $D_{(s)}^+ \rightarrow h^+\mu^+\mu^-$ ,

$D^0 \rightarrow hh'\mu^+\mu^-$  are likewise interesting. The former modes have long-distance contributions of order  $10^{-6}$  from vector intermediaries ( $\rho, \omega, \phi$ ) but these can be cut away. The standard model rate for the remaining decays is around  $10^{-11}$ . For the latter modes, one can form forward-backward and  $T$ -odd asymmetries with sensitivity to new physics.

Experimentally, at present, there are only the upper limits on  $D^0 \rightarrow \ell^+\ell^-$  decays,

$$\mathcal{B}(D^0 \rightarrow \mu^+\mu^-) \leq 1.1 \times 10^{-8}, \quad \mathcal{B}(D^0 \rightarrow e^+e^-) \leq 7.9 \times 10^{-8}, \quad \mathcal{B}(D^0 \rightarrow \mu^\pm e^\mp) \leq 2.6 \times 10^{-7}. \quad (14)$$

Theoretically, just like in the case of mixing discussed above, all possible NP contributions to  $c \rightarrow u\ell^+\ell^-$  can also be summarized in an effective Hamiltonian,

$$\mathcal{H}_{\text{NP}}^{\text{rare}} = \sum_{i=1}^{10} \tilde{C}_i(\mu) \tilde{Q}_i, \quad \begin{aligned} \tilde{Q}_1 &= (\bar{\ell}_L \gamma_\mu \ell_L) (\bar{u}_L \gamma^\mu c_L), & \tilde{Q}_4 &= (\bar{\ell}_R \ell_L) (\bar{u}_R c_L), \\ \tilde{Q}_2 &= (\bar{\ell}_L \gamma_\mu \ell_L) (\bar{u}_R \gamma^\mu c_R), & \tilde{Q}_5 &= (\bar{\ell}_R \sigma_{\mu\nu} \ell_L) (\bar{u}_R \sigma^{\mu\nu} c_L), \\ \tilde{Q}_3 &= (\bar{\ell}_L \ell_R) (\bar{u}_R c_L), \end{aligned} \quad (15)$$

where  $\tilde{C}_i$  are again Wilson coefficients, and the  $\tilde{Q}_i$  are the effective operators. In this case, however, there are ten of them, with five additional operators  $\tilde{Q}_6, \dots, \tilde{Q}_{10}$  that can be obtained from operators in Eq. (15) by the substitutions  $L \rightarrow R$  and  $R \rightarrow L$ . Further details may be found in Ref. [108], where it is also noted that it might be advantageous to study correlations of new physics contributions to various processes, for instance  $D^0 - \bar{D}^0$  mixing and rare decays.

## Strong Phases

Threshold data with correlated  $D^0 - \bar{D}^0$  pairs may be used to extract strong phases in  $D$  decays. These phases enter into  $B$  physics determinations of the CKM angle  $\gamma$  from  $B \rightarrow D^{(*)}K^{(*)}$  decays [109]. Without direct input from charm, these  $B$  results suffer from ill-defined systematic uncertainties and lose precision. In addition, strong phases are needed to relate observables of  $D^0 - \bar{D}^0$  oscillations measured with hadronic final states to the usual  $x, y$  parameters.

## Charmonium Spectroscopy

In the last decade, the observations of the spin-singlet charmonium states  $h_c(1P)$  and  $\eta_c(2S)$  have completed the charmonium multiplets below the open-charm threshold. Experiments have also revealed a large number of unexpected  $c\bar{c}$  mesons above the open-charm threshold, labelled  $XYZ$  states. These states may include tetraquarks,  $c\bar{c}g$  hybrids, meson molecules, etc. Many of the  $XYZ$  states are narrow and some are manifestly exotic, indicating a gap in our understanding of the QCD spectrum. Understanding their spectrum and decays are major challenges for lattice QCD and phenomenology. Experimental data on the  $XYZ$  states continues to accumulate, and more can be expected from future experiments. The challenge of charmonium spectroscopy above the open-charm threshold is discussed in detail in a Snowmass White Paper [55].

## Other Topics

We finally list a few topics on “engineering numbers.” Currently, charm lifetimes are dominated by FOCUS results; while the results are well-respected, a cross-check would be welcome. These results serve to relate theoretical predictions for partial widths to the experimentally accessible quantities, branching fractions.

Likewise, golden mode branching fractions for  $D$  mesons are dominated by CLEO-c; a cross-check from BESIII is in order. For the baryons, where there are four weakly-decaying ground states, there are no absolute branching fraction results. For  $\Lambda_c \rightarrow pK^- \pi^+$ , the near-threshold enhancement of  $\Lambda_c$  pairs measured by Belle in ISR [110] shows that BESIII should be able to provide a nice result with a modest-length run.

In addition to topics discussed above, charm quarks will play a major role in the heavy-ion experimental programs at RHIC and LHC for the next decade. Questions that will be addressed include identification of the exact energy loss and hadronization mechanisms of charm (or beauty) quarks in propagation through Quark-Gluon Plasma (QGP), calculations of heavy quark transport coefficients, etc.

### 5.3 Charm Physics Summary and Perspectives Beyond 2020

Continued support of BESIII, LHCb, and Belle II is critical to U.S. involvement in a vibrant charm program. Investments in these provide valuable access to exciting datasets. Attention should also be paid to possible opportunities at a future threshold experiment should one be built abroad.

Theoretical calculations in charm physics are mainly driven by experimental results. The challenges associated with nonperturbative QCD dynamics are being addressed by advances in lattice QCD and other nonperturbative approaches. While similar probes of the NP scale that might reveal the “grand design” of flavor are available in the strange and beauty systems, charm quarks furnish unique access to processes involving up quarks, more precise and complementary to searches for FCNC top decays. Moreover,  $D$  mesons are the only neutral mesons composed of up-type quarks which have flavor oscillations, and thus probe NP in the  $\Delta F = 2$  transitions, providing complementary sensitivity to  $K$ ,  $B$ , and  $B_s$  mixing.

## 6 Report of the Lattice QCD Task Force

The properties of the five least massive quarks offer a powerful tool to indirectly study physics at energies many orders of magnitude above those which are directly accessible to present or planned accelerators. This is made possible in large part by the quarks’ strong interactions which provide experimental physics with a host of bound states, common and rare decay processes and mixings that enable clever and highly sensitive studies of the properties of the underlying quarks. Until recently, the lack of predictive control of these same strong interactions provided a large barrier to fully exploiting this potential. Ab initio lattice calculations are systematically removing this barrier, allowing us to fully exploit the strong interactions of the quarks to search for physics beyond the standard model. In this section we describe the status and prospects for the lattice QCD calculations needed for future quark-flavor experiments. Much of this material is drawn from a recent USQCD (the national U.S. lattice-QCD collaboration) white paper [111].

Lattice QCD provides a first-principles method for calculating low-energy hadronic matrix elements with reliable and systematically-improvable uncertainties. Such matrix elements — decay constants, form factors, mixing matrix elements, etc. — are needed to determine the standard model (SM) predictions for many processes and/or to extract CKM matrix elements.

In the last five years lattice QCD has matured into a precision tool. Results with fully controlled errors are available for nearly 20 matrix elements: the decay constants  $f_\pi$ ,  $f_K$ ,  $f_D$ ,  $f_{D_s}$ ,  $f_B$  and  $f_{B_s}$ , semileptonic form factors for  $K \rightarrow \pi$ ,  $D \rightarrow K$ ,  $D \rightarrow \pi$ ,  $B \rightarrow D$ ,  $B \rightarrow D^*$ ,  $B_s \rightarrow D_s$  and  $B \rightarrow \pi$ , and the four-fermion mixing matrix elements  $B_K$ ,  $f_B^2 B_B$  and  $f_{B_s}^2 B_{B_s}$ . By contrast, in 2007 (when the previous USQCD white paper was



Quantity	CKM element	Present expt. error	2007 forecast lattice error	Present lattice error	2018 lattice error
$f_K/f_\pi$	$ V_{us} $	0.2%	0.5%	0.4%	0.15%
$f_+^{K\pi}(0)$	$ V_{us} $	0.2%	–	0.4%	0.2%
$f_D$	$ V_{cd} $	4.3%	5%	2%	< 1%
$f_{D_s}$	$ V_{cs} $	2.1%	5%	2%	< 1%
$D \rightarrow \pi \ell \nu$	$ V_{cd} $	2.6%	–	4.4%	2%
$D \rightarrow K \ell \nu$	$ V_{cs} $	1.1%	–	2.5%	1%
$B \rightarrow D^* \ell \nu$	$ V_{cb} $	1.3%	–	1.8%	< 1%
$B \rightarrow \pi \ell \nu$	$ V_{ub} $	4.1%	–	8.7%	2%
$f_B$	$ V_{ub} $	9%	–	2.5%	< 1%
$\xi$	$ V_{ts}/V_{td} $	0.4%	2–4%	4%	< 1%
$\Delta m_s$	$ V_{ts}V_{tb} ^2$	0.24%	7–12%	11%	5%
$B_K$	$\text{Im}(V_{td}^2)$	0.5%	3.5–6%	1.3%	< 1%

**Table 6.** History, status and future of selected lattice-QCD calculations needed for the determination of CKM matrix elements. 2007 forecasts are from Ref. [112]. Most present lattice results are taken from [latticeaverages.org](http://latticeaverages.org) [113]. The quantity  $\xi$  is  $f_{B_s} \sqrt{B_{B_s}} / (f_B \sqrt{B_B})$ .

written [112]), only  $f_K/f_\pi$  was fully controlled. A sample of present errors is collected in Table 6. For  $K$  mesons, errors are at or below the percent level, while for  $D$  and  $B$  mesons errors range from few to  $\sim 10\%$ .

The lattice community is embarking on a three-pronged program of future calculations: (i) steady but significant improvements in “standard” matrix elements of the type just described, leading to much improved results for CKM parameters (e.g.,  $V_{cb}$ ); (ii) results for many additional matrix elements relevant for searches for new physics and (iii) the extension of lattice methods to more challenging matrix elements which can both make use of old results and provide important information for upcoming experiments.

Reducing errors in the standard matrix elements has been a major focus of the lattice community over the last five years, and the improved results illustrated in Table 6 now play an important role in the determination of the CKM parameters in the “unitarity triangle fit.” Lattice-QCD calculations involve various sources of systematic error (the need for extrapolations to zero lattice spacing, infinite volume and the physical light-quark masses, as well as fitting and operator normalization) and thus it is important to cross-check results using multiple discretizations of the continuum QCD action. (It is also important to check that results for the hadron spectrum agree with experiment. Examples of these checks are shown in the 2013 whitepaper [111].) This has been done for almost all the quantities noted above. This situation has spawned two lattice averaging efforts, [latticeaverages.org](http://latticeaverages.org) [113] and FLAG-1 [114], which have recently joined forces and expanded to form a worldwide Flavor Lattice Averaging Group (FLAG-2), with first publication expected in mid-2013.

The ultimate aim of lattice-QCD calculations is to reduce errors in hadronic quantities to the level at which they become subdominant either to experimental errors or other sources of error. As can be seen from Table 6, several kaon matrix elements are approaching this level, while lattice errors remain dominant in most quantities involving heavy quarks. Thus the most straightforward contribution of lattice QCD to the future intensity frontier program will be the reduction in errors for such quantities. Forecasts for the expected reductions by 2018 are shown in the table. These are based on a Moore’s law increase in computing power,

and extrapolations using existing algorithms. Past forecasts have been typically conservative (as shown in the table) due to unanticipated algorithmic or other improvements. The major reasons for the expected reduction in errors are the use of  $u$  and  $d$  quarks with physical masses, the use of smaller lattice spacings and improved heavy-quark actions, and the reduction in statistical errors.

Thus one key contribution of lattice QCD to the future flavor-physics program will be a significant reduction in the errors in CKM elements, most notably  $V_{cb}$ . This feeds into the SM predictions for several of the rare decays that are part of the proposed experimental program, e.g.,  $K \rightarrow \pi\nu\bar{\nu}$ . For these decays, the parametric error from  $|V_{cb}|$ , which enters as the fourth power, is the dominant source of uncertainty in the SM predictions. The lattice-QCD improvements projected in Table 6 will bring the theoretical uncertainties to a level commensurate with the projected experimental errors in time for the planned rare kaon-decay experiments at Fermilab.

The matrix elements discussed so far involve only a single hadron and no quark-disconnected contractions. These are the most straightforward to calculate (and are sometimes called “gold-plated”). The second part of the future lattice-QCD program for the intensity frontier will be the extension of the calculations to other, similar, matrix elements which are needed for the search for new physics. This includes the mixing matrix elements for kaons,  $D$  and  $B$  mesons arising from operators present in BSM theories but absent in the SM, the form factors arising in  $B \rightarrow K\ell^+\ell^-$  and  $\Lambda_b \rightarrow \Lambda\ell^+\ell^-$ , non-SM form factors for  $K \rightarrow \pi$ ,  $B \rightarrow \pi$  and  $B \rightarrow K$  transitions. We expect the precision attained for these quantities to be similar to those for comparable quantities listed in Table 6.

The third part of the lattice-QCD program is the least developed and most exciting. This involves the development of new methods or the deployment of known but challenging methods, and allows a substantial increase in the repertoire of lattice calculations. In particular, calculations involving two particles below the inelastic threshold are now possible (e.g.,  $K \rightarrow \pi\pi$  amplitudes [115, 116, 117]), quark-disconnected contractions are being controlled (e.g.,  $\eta'$  and  $\eta$  masses [118] and the nucleon sigma term [119]) and processes involving two insertions of electroweak operators are under pilot study (e.g., the long-distance part of  $\Delta m_K$  [120]). During the next five years, we expect that these advances will lead to a quantitative understanding of the  $\Delta I = 1/2$  rule, a prediction with  $\sim 5\%$  errors for the the SM contribution to  $\epsilon'_K$ , and predictions with 10–20% errors for the long-distance contributions to  $\Delta m_K$  and  $\epsilon_K$ . This will finally allow us to use these hallowed experimental results in order to search for new physics.

These new methods should allow lattice QCD to contribute directly to the proposed flavor-physics experiments. For example, a calculation of the long-distance contributions to  $K \rightarrow \pi\nu\bar{\nu}$  decays should be possible, checking the present estimate that these contributions are small. Similar methods should allow the calculation of the sign of the CP-conserving amplitude  $K_S \rightarrow \pi^0 e^- e^+$ , thus resolving a major ambiguity in the SM prediction for  $K_L \rightarrow \pi^0 e^- e^+$ .

We also expect progress on even more challenging calculations, for which no method is yet known. An important example, in light of recent evidence for CP violation in  $D$  decays and for  $D - \bar{D}$  mixing, is to develop a method for calculating the amplitudes for  $D \rightarrow \pi\pi$ ,  $KK$  decays and  $D - \bar{D}$  mixing. This requires dealing with four or more particles in a finite box, as well as other technical details.

These plans rely crucially on access to high-performance computing, as well as support for algorithm and software development. In the U.S., much of this infrastructure is coordinated by the USQCD umbrella collaboration. Continued support for this effort is essential for the program discussed here.

We also stress that there are substantial lattice-QCD efforts underway to calculate the hadronic (vacuum polarization and light-by-light) contributions to muonic  $g - 2$ , the light- and strange-quark contents of the nucleon (which are needed to interpret  $\mu \rightarrow e$  conversion and dark-matter experiments), and the nucleon axial form factor (which enters the determination of the neutrino flux at many accelerator-based neutrino

experiments). Smaller-scale lattice-QCD calculations of nucleon EDMs, proton- and neutron-decay matrix elements, and neutron-antineutron oscillation matrix elements are also in progress. These are very important for the intensity frontier as a whole, although not directly relevant to quark-flavor physics.

In the remainder of this subsection, we describe the major new efforts that are underway or envisaged for the next 5 or so years, considering in turn kaons,  $D$  mesons and  $B$  mesons, and close with a 15-year vision.

## 6.1 Future Lattice Calculations of Kaon Properties

**$K \rightarrow \pi\pi$  amplitudes:** These amplitudes are now active targets of lattice-QCD calculations. The final-state pions can be arranged to have physical, energy-conserving relative momentum by imposing appropriate boundary Corrections for the effects of working in finite volume can be made following the analysis of Ref. [121]. A first calculation of the amplitude to the  $I = 2$  two-pion state,  $A_2$ , has been performed [115] with physical kinematics but 15% finite lattice spacing errors. Calculations are now underway using two ensembles with smaller lattice spacings which will allow a continuum extrapolation, removing this error. Results with an overall systematic error of  $\approx 5\%$  are expected within the coming year.

The calculation of  $A_0$  is much more difficult because of the overlap between the  $I = 0$   $\pi\pi$  state and the vacuum, resulting in disconnected diagrams and a noise to signal ratio that grows exponentially with time separation. In addition, for  $I = 0$ ,  $G$ -parity boundary conditions must be employed and imposed on both the valence and sea quarks. These topics have been actively studied for the past three years [122] and  $G$ -parity boundary conditions successfully implemented [123]. First results with physical kinematics are expected within two years from a relatively coarse,  $32^3 \times 64$  ensemble. Errors on  $\epsilon'_K$  on the order of 15% should be achieved, with the dominant error coming from the finite lattice spacing. As in the case of the easier  $A_2$  calculation, lessons learned from this first, physical calculation will then be applied to calculations using a pair of ensembles with two lattice spacings so that a continuum limit can be obtained. A five-year time-frame may be realistic for this second phase of the calculation. Essential to the calculation of both  $A_0$  and  $A_2$  is the renormalization of the lattice operators. Significant efforts will be required in the next 2–3 years to extend the range of nonperturbative renormalization methods up through the charm threshold and to a scale of 4–5 GeV where perturbative matching to the conventional  $\overline{\text{MS}}$  scheme will have small and controlled errors.

**Long-distance contributions to  $\Delta m_K$  and  $\epsilon_K$ :** Promising techniques have been developed which allow the calculation of the long-distance contribution to kaon mixing by lattice methods. By evaluating a four-point function including operators which create and destroy the initial and final kaons and two effective weak four-quark operators, the required second order amplitude can be explicitly evaluated. Integrating the space-time positions of the two weak operators over a region of fixed time extent  $T$  and extracting the coefficient of the term which grows linearly with  $T$  gives precisely both  $\Delta m_K$  and  $\epsilon_K$ . This Euclidean space treatment of such a second-order process contains unphysical contributions which grow exponentially with  $T$  and must be subtracted. The statistical noise remaining after this subtraction gives even the connected diagrams the large-noise problems typical of disconnected diagrams. Preliminary results suggest that this problem can be solved by variance reduction methods and large statistics [120]. Given the central importance of GIM cancellation in neutral kaon mixing, a lattice calculation that is not burdened by multiple subtractions must include the charm quark mass with consequent demands that the lattice spacing be small compared to  $1/m_c$  — a substantial challenge for a calculation which should also contain physical pions in an appropriately large volume. Perturbative results [124] as well as the first lattice calculation [120] suggest that perturbation theory works poorly at energies as low as the charm mass, making the incorporation of charm in a lattice calculation a high priority. Given the challenge of including both physical pions and active charm quarks,

the first calculation of  $\Delta m_K$  may take 4–5 years. Results for the long-distance part of  $\epsilon_K$  may be obtained in a similar time frame. However, a more challenging subtraction procedure must be employed for  $\epsilon_K$ .

**Rare kaon decays:** Given the promise of the first calculations of the long distance contributions to  $\Delta m_K$ , a process that involves two  $W^\pm$  exchanges, it is natural to consider similar calculations for the second-order processes which enter important rare kaon decays such as  $K_L^0 \rightarrow \pi^0 \ell^+ \ell^-$  and  $K^+ \rightarrow \pi^+ \nu \bar{\nu}$ . While in principle  $K_L \rightarrow \ell^+ \ell^-$  should also be accessible to lattice methods, the appearance of three electroweak, hadronic vertices suggests that this and similar processes involving  $H_W^{\Delta S=1}$  and two photons, should be tackled only after success has been achieved with more accessible, second order processes.

The processes  $K^+ \rightarrow \pi^+ \nu \bar{\nu}$  and  $K_L \rightarrow \pi^0 \nu \bar{\nu}$  may be the most straightforward generalization of the current  $\Delta m_K$  calculation. Here the dominant contribution comes from box and  $Z$ -penguin diagrams involving top quarks, but with a 30% component of the CP-conserving process coming from the charm quark [125]. While the charm quark piece is traditionally referred to as “short distance,” the experience with  $\Delta m_K$  described above suggests that a nonperturbative evaluation of this charm-quark contribution may be a necessary check of the usual perturbative approach, which is here believed to be reliable. There are also “longer distance” contributions which are only accessible to lattice methods and will become important when the accuracy of rare kaon decay experiments reaches the 3% level, or possibly sooner. The long-distance contributions to the decay  $K_{L/S} \rightarrow \pi^0 \ell^+ \ell^-$  also appear to be a natural target for a lattice-QCD calculation since the sign of the CP-conserving process  $K_S \rightarrow \pi^0 \ell^+ \ell^-$  may be only determined this way.

## 6.2 Future Lattice Calculations of $D$ -meson Properties

**$D \rightarrow \pi\pi$ ,  $KK$  amplitudes:** Recent experimental evidence suggests that there may be CP violation in  $D \rightarrow \pi\pi$  and  $D \rightarrow KK$  decays. In order to interpret these results, it is essential to be able to predict the CP violation expected in the SM. Even a result with a large, but reliable, error could have a large impact. This need will become even more acute over the next five years as LHCb and Belle II improve the measurements.

This calculation is more challenging than that for  $K \rightarrow \pi\pi$  decays, which represent the present frontier of lattice calculations. In the kaon case, one must deal with the fact that two-pion states in finite volume are not asymptotic states, and the presence of multiple quark-disconnected contractions. For  $D$  decays, even when one has fixed the strong-interaction quantum numbers of a final state (say to  $I = S = 0$ ), the strong interactions necessarily bring in multiple final states:  $\pi\pi$  and  $K\bar{K}$  mix with  $\eta\eta$ ,  $4\pi$ ,  $6\pi$ , etc. The finite-volume states used by lattice QCD are inevitably mixtures of all these possibilities, and one must learn how, in principle and in practice, to disentangle these states to obtain the desired matrix element. Recently, a first step towards developing a complete method has been taken [126], in which the problem has been solved in principle for any number of two-particle channels, and assuming that the scattering is dominantly  $S$  wave. This is encouraging, and this method may allow one to obtain semi-quantitative results for the amplitudes of interest. We expect that turning this method into practice will take  $\sim 5$  years due to a number of numerical challenges (in particular the need to calculate several energy levels with good accuracy).

In the more distant future, we expect that it will be possible to generalize the methodology to include four-particle states; several groups are actively working on the theoretical issues and much progress has been made already for three particles.

**$D - \bar{D}$  mixing:** Mixing occurs in the  $D^0 - \bar{D}^0$  system, and there is no evidence yet for CP violation in this mixing [62]. The short-distance contributions can be calculated for  $D$  mesons using lattice QCD, as for kaons and  $B$  mesons. The challenge, however, is to calculate the long-distance contributions. As in the case of  $\Delta m_K$  discussed above, there are two insertions of the weak Hamiltonian, with many allowed

states propagating between them. The  $D$  system is much more challenging, however, since, as for the decay amplitudes, there are many strong-interaction channels having  $E < m_D$ . Further theoretical work is needed to develop a practical method.

### 6.3 Future Lattice Calculations of $B$ -meson Properties

**$B \rightarrow D^{(*)}\ell\nu$  form factors at nonzero recoil:** Lattice-QCD results for these form factors allow for the determination of  $|V_{cb}|$  from the measured decay rates. For the  $B \rightarrow D^*\ell\nu$  form factor at zero recoil, the gap between experimental errors (1.3%) and lattice errors (currently  $\sim 1.8\%$ ) has narrowed considerably over the last five years. In the next five years, we expect the lattice contribution to the error in  $|V_{cb}|$  to drop below the experimental one, as shown in Table 6. Particularly important for this will be the extension of the  $B \rightarrow D^{(*)}\ell\nu$  form-factor calculations to nonzero recoil [127].

**Tauonic  $B$ -decay matrix elements:** Recently the *BABAR* collaboration measured the ratios  $R(D^{(*)}) = \mathcal{B}(B \rightarrow D^{(*)}\tau\nu)/\mathcal{B}(B \rightarrow D^{(*)}\ell\nu)$  with  $\ell = e$  or  $\mu$ , and observed a combined excess over the existing SM predictions of  $3.4\sigma$  [128]. Those SM predictions were based, however, on models of QCD, not *ab initio* QCD. Realizing that it was much easier to obtain accurate results for these ratios than for the form factors themselves, the Fermilab-MILC collaboration responded quickly (using lattice data already in hand), and provided the first lattice-QCD result for  $R(D)$  [129]. Their result slightly reduced the discrepancy with experiment for  $R(D)$  from  $2.0 \rightarrow 1.7\sigma$ . At present, the experimental errors in  $R(D)$  ( $\sim 16\%$ ) dominate over lattice errors (4.3%), so further lattice improvements are not needed in the short run. The experimental uncertainties will shrink with the increased statistics available at Belle II, and it should be straightforward to reduce the corresponding lattice-QCD error by a factor of two over the next five years. Work is also in progress to calculate  $R(D^*)$ , for which the uncertainties are expected to be comparable to those of  $R(D)$ .

Belle II will also reduce the uncertainty in the experimental measurement of  $\mathcal{B}(B \rightarrow \tau\nu)$  to the few-percent level with its anticipated full data set. In the next five years, lattice-QCD calculations are expected to reduce the error in  $f_B$  to the percent level (see Table 6). Particularly important for this will be the use of finer lattice spacings that permit relativistic  $b$ -quark actions [130]. Combined with the anticipated experimental precision, this will increase the reach of new-physics searches in  $B \rightarrow \tau\nu$ ; moreover, correlations between  $B \rightarrow \tau\nu$  and  $B \rightarrow D^{(*)}\tau\nu$  decays can help distinguish between new-physics models.

**$B \rightarrow K\ell^+\ell^-$  and related decay form factors:** The branching ratio for  $B \rightarrow K\ell^+\ell^-$  is now well measured, and increasingly accurate results from LHCb, and eventually Belle II, are expected. The SM prediction requires knowledge of the vector and tensor  $b \rightarrow s$  form factors across the kinematic range. Present theoretical estimates use light-cone sum rules, but several first-principles lattice-QCD calculations are nearing completion, as reviewed in Ref. [131]. The calculation is similar to that needed for the  $B \rightarrow \pi\ell\nu$  form factor, and we expect similar accuracy to be obtained over the next five years.

A related process is the baryonic decay  $\Lambda_b \rightarrow \Lambda\ell^+\ell^-$ , recently measured by CDF. Here the extra spin degree of freedom can more easily distinguish between SM and BSM contributions. A lattice-QCD calculation of the required form factors has recently been completed, using HQET to describe the  $b$  quark [132]. Errors of  $\sim 10\text{--}15\%$  in the form factors are obtained, which are comparable to present experimental errors. The latter errors will decrease with new results from LHCb, and so improved LQCD calculations and cross-checks are needed. Although the calculation is conceptually similar to that for  $B \rightarrow K\ell^+\ell^-$ , given the presence of baryons we expect the errors for  $\Lambda_b \rightarrow \Lambda\ell^+\ell^-$  to lag somewhat behind.

**Non-standard model form factors for  $K \rightarrow \pi$  and  $B \rightarrow \pi$  transitions:** The  $B \rightarrow K$  vector and tensor form factors just discussed are also needed to describe decays involving missing energy,  $B \rightarrow KX$ , in

BSM theories [33]. Analogous form factors are needed for  $B \rightarrow \pi X$  and  $K \rightarrow \pi X$  decays. The tensor form factors are also needed to evaluate some BSM contributions to  $K \rightarrow \pi \ell^+ \ell^-$  [133]. Thus it is of interest to extend the present calculations of vector form factors in  $K \rightarrow \pi$  and  $B \rightarrow \pi$  to include the tensor matrix elements. Since these are straightforward generalizations of present calculations, we expect that comparable accuracy to the present errors in Table 6 can be obtained quickly, and that future errors will continue to follow the projections for similar matrix elements.

## 6.4 Lattice QCD and Flavor Physics: 2018–2030

The discussion above has laid out an ambitious vision for future lattice-QCD calculations on a five-year timescale, explaining how they can provide essential information for upcoming quark-flavor experiments. Also discussed are a number of more challenging quantities which have become accessible to lattice methods only recently. In this section we discuss more generally the opportunities offered by lattice methods over the extended time period covered by the Snowmass study. However, we should emphasize that these longer range forecasts are made difficult by the very rapid evolution of this emerging field, which is driven by both rapidly advancing commercial computer technology and continual, difficult-to-anticipate advances in algorithms.

We begin with the conservative assumptions that exascale performance ( $10^{18}$  floating point operations/second) will be achieved by 2022, and that a further factor of 100 will be available by 2032. These represent factors of  $10^2$  and  $10^4$  over presently available capability. At fixed physical quark masses, the difficulty of modern lattice-QCD algorithms scales with decreasing lattice spacing  $a$  as  $1/a^6$  and with increasing physical linear problem size  $L$  as  $L^5$ . Present large-scale lattice calculations at physical quark masses are performed in volumes of linear size  $L \approx 6$  fm and with inverse lattice spacing  $1/a$  as small as  $\sim 2.5$  GeV. Thus, these  $10^2$  and  $10^4$  advances in computer capability will allow an increase in physical volume to 15 and 36 fm and in inverse lattice spacing to 5 and 10 GeV, respectively. Statistical errors can be reduced from their present percent-level for many quantities to 0.1% or even 0.01% as needed.

These three directions of substantial increase in capability translate directly into physics opportunities. The large increase in possible Monte Carlo statistics is necessary if we are to decrease the errors on many of the quantities in Table 6 to the 0.1% level. Such increased statistics will also directly support perhaps 1% precision for results that depend on disconnected diagrams such as  $\epsilon'_K$  and the  $K_L - K_S$  mass difference. For most QCD calculations, the non-zero pion mass implies that finite volume effects decrease exponentially in the linear size of the system. However, this situation changes dramatically when electromagnetic effects are included. Here the massless photon and related difficulties of dealing with charged systems in finite volume result in substantial finite volume errors which decrease only as a power of  $L$  as the linear system size  $L$  becomes large. The ability to work on systems of linear size 20 or 30 fm will play an important role in both better understanding electromagnetic effects using lattice methods and achieving the 10% errors in the computation of such effects that are needed to attain 0.1% errors in many of the quantities in Table 6.

Finally the ability to work with an inverse lattice spacing as large as 10 GeV will allow substantial improvements in the treatment of heavy quarks. Using  $3 \text{ GeV} \leq 1/a \leq 5 \text{ GeV}$ , calculations involving charm quarks will have controlled finite lattice spacing errors on the 1% level or smaller. As a result calculation of the long-distance contributions, up to and including the charm scale, will be possible for  $\Delta m_K$ ,  $\epsilon_K$  and rare kaon decays yielding errors of order 1% for these important quantities. The larger inverse lattice spacings in the range  $6 \text{ GeV} \leq 1/a \leq 10 \text{ GeV}$  will allow the present estimates of the finite lattice spacing errors in bottom quark systems to both be substantially reduced and to be refined using the new information provided by a larger range of lattice spacings. This will allow many quantities involving bottom quarks to be determined with errors well below 1%.

While ever more difficult to forecast, a  $10^4$  increase in capability can be expected to significantly expand the range of quantities that can be computed using lattice methods. These include the  $D - \bar{D}$  mixing and multi-particle  $D$  decays discussed in the previous section as well as even more challenging quantities such as semileptonic  $B$  decays with vector mesons in the final state. These are relevant both for the extraction of CKM matrix elements (e.g.,  $B \rightarrow \rho \ell \nu$  provides an alternative determination of  $|V_{ub}|$ ) and new-physics searches (e.g., measurements of  $B \rightarrow K^* \ell^+ \ell^-$ ,  $B \rightarrow K^* \gamma$  and  $B_s \rightarrow \phi \gamma$ ). A second example is nonleptonic  $B$  decays, such as  $B \rightarrow D\pi(K)$ , which can be used to obtain the CKM angle  $\gamma$ .

Clearly an enhanced computational capability of four orders of magnitude, coupled with possibly equally large advances in numerical algorithms, will have a dramatic effect on the phenomena that can be analyzed and precision that can be achieved using lattice methods. The possibility of making SM predictions with errors which are an order of magnitude smaller than present experimental errors will create an exciting challenge to identify quantities where substantially increased experimental accuracy is possible and where the impact of such measurements on the search for physics beyond the SM most sensitive. With the ability to make highly accurate SM predictions for a growing range of quantities, experiments can be designed that will achieve the greatest precision for quantities sensitive to physics beyond the SM, rather than being limited to those quantities which are least obscured by the effects of QCD.

## 7 A U.S. Plan for Quark Flavor Physics

Until recently, the U.S. had onshore accelerator facilities that supported a leadership role at both the Energy and Intensity Frontiers. With the successful start of the LHC and the termination of the Tevatron program, the Energy Frontier has migrated offshore for the foreseeable future. With choices summarized in Section 1, the U.S. ceded leadership in much of quark-flavor physics. It is difficult to foresee a scenario that leads to the construction of a facility in the U.S. that is capable of supporting  $B$ -physics or charm-physics experiments during the current decade or even the next decade. Indeed, the only accelerator-based experiments currently in the DOE pipeline are neutrino experiments and muon experiments at Fermilab, and to achieve their full potential these experiments depend on Fermilab's *Project X* facility, which has yet to achieve the first level of DOE approval ("mission need"). It is under these rather dire circumstances, facing the prospect that the U.S. accelerator-based HEP program may go the way of the dodo bird, that we must contemplate the question of whether and how the U.S. should pursue research in quark-flavor physics.

There is a strong physics case for quark-flavor physics that remains robust in all LHC scenarios. It rests, quite simply, on the potential of precision quark-flavor experiments and studies of very rare decays to observe the effect of high-mass virtual particles. If new physics is observed at LHC, tighter constraints from the flavor sector will narrow the range of models that can account for the observed states. If new physics is not discovered at LHC, then the reach to mass scales beyond that of LHC will still offer the potential to find new physics and to estimate the scale needed for direct observation. International recognition of the importance of quark-flavor physics is evident from the commitments in Europe and Asia to conduct the next-generation of  $B$ -physics, charm, and kaon experiments.

In the U.S., the goal should be to construct an HEP program that has the breadth to assure meaningful participation in making the discoveries that will define the future of particle physics. The successful U.S. contributions to LHC have demonstrated that physicists from U.S. laboratories and universities can play essential roles in offshore experiments. If this paradigm works at the Energy Frontier, it can work at the Intensity Frontier as well. Therefore, significant U.S. contributions to offshore quark-flavor experiments such as LHCb and Belle II should be encouraged. Also, in the one area where existing and foreseeable facilities on U.S. soil can support a world-leading program — kaon physics — the U.S. should embrace the opportunity. The accelerator facilities required for kaon experiments are exactly those needed for the neutrino program,

so the costs are incremental and relatively modest. Below, we summarize the opportunities that exist now and those that will exist during the next decade.

## 7.1 Opportunities in This Decade

The Task Force reports have described current, planned, and possible  $B$ -physics, charm, and kaon experiments in Europe and Asia. There is a strong and diverse international program. The only U.S. entry in the discussion of the immediate future for quark-flavor physics experiments is the ORKA proposal at Fermilab, for an experiment which would make a precise measurement of the  $K^+ \rightarrow \pi^+ \nu \bar{\nu}$  branching fraction.

For the remainder of this decade, the plans in Europe and Asia appear to be set, and the experiments there (those already running or under construction) will define the frontier of quark-flavor physics. These are LHCb and NA62 at CERN, KLOE2 in Italy, PANDA in Germany, BESIII in China, and Belle II, KOTO, and TREK in Japan. This is a rich program, and fortunately U.S. physicists have some involvement in most of these experiments. While they all have important physics goals and capabilities, the scale of LHCb and Belle II, and their incredibly broad physics menus including both bottom and charm, means that they will be the flagship experiments in quark-flavor physics. In view of that, the U.S. should try to play a significant role in these experiments.

The outstanding question is whether the ORKA experiment will go forward at Fermilab. It received “Stage 1” approval from Fermilab in the fall of 2011, but has not been integrated into DOE’s planned program thus far. A clear conclusion of this Snowmass working group is that ORKA presents an extraordinary opportunity. If the U.S. HEP program endeavors to achieve a leading role at the Intensity Frontier, ORKA should be pursued.

In short, the optimal U.S. plan in quark-flavor physics for the remainder of this decade has four elements.

- U.S. physicists should be supported to carry out significant roles in LHCb and Belle II.
- The ORKA experiment should move forward in a timely way at Fermilab.
- Support for U.S. participation on other experiments that are in progress (e.g., KOTO, TREK, BESIII) should be maintained.
- Support for theory, and the computing facilities needed for lattice QCD, should be maintained.

## 7.2 Opportunities in the Next Decade

In the decade beginning around 2020, we can anticipate that LHCb will be well on its path toward collecting  $50 \text{ fb}^{-1}$  and Belle II will be well on its path toward  $50 \text{ ab}^{-1}$ . These will be complementary data samples, overlapping in some areas but providing different strengths in others. We anticipate that the U.S. HEP program will be continuing its emphasis on Intensity Frontier experiments, with a commitment to providing high-intensity proton sources for the production of neutrino beams for neutrino experiments. If so, the potential for such a high-intensity proton source to support the next generation of rare kaon decay experiments is an opportunity unique to the U.S. program. In particular, *Project X* at Fermilab can deliver more than an order of magnitude increase in the beam power available for producing kaons compared to any other laboratory in the world. In addition, the CW-linac of *Project X* can provide a time structure that is programmable bunch-by-bunch. That capability can be exploited in neutral kaon experiments to



measure the momentum of individual  $K_L^0$ 's via time-of-flight, opening the door to dramatic improvements in background rejection for some challenging rare decays.

*Project X* can be the leading facility in the world for rare kaon decay experiments.

### 7.3 Conclusions

This report has described the physics case for precision studies of flavor-changing interactions of bottom, charm, and strange quarks, and it has described the experimental programs that are underway and foreseeable around the world. A substantial number of physicists in the U.S. are motivated to work in this area, both theorists and experimentalists. Quark-flavor physics should be a component in the plan for the future U.S. HEP program.

After enduring the full “Snowmass process,” the Quark Flavor Physics working group has produced this report. It reflects a wide range of inputs. Its contents and conclusions have been publicly vetted. For instance, drafts of this report were posted for two rounds of public comment.

Our major conclusions can be summarized as follows:

- Quark flavor physics is an essential element in the international high-energy physics program. Experiments that study the properties of highly suppressed decays of strange, charm, and bottom quarks have the potential to observe signatures of new physics at mass scales well beyond those directly accessible by current or foreseeable accelerators.
- The importance of quark flavor physics is recognized in Europe and Asia, as demonstrated by the commitments to LHCb, NA62, KLOE-2, and Panda in Europe, and to Belle II, BESIII, KOTO, and TREK in Asia.
- In order for the U.S. HEP program to have the breadth to assure meaningful participation in future discoveries, significant U.S. contributions to offshore quark-flavor experiments is important, and continued support for U.S. groups in these efforts is a sound investment. In particular, U.S. contributions to LHCb and Belle II should be encouraged because of the richness of the physics menus of these experiments and their reach for new physics.
- Existing facilities at Fermilab are capable of mounting world-leading rare kaon decay experiments in this decade at modest incremental cost to running the Fermilab neutrino program. The proposed ORKA experiment, to measure the rare decay  $K^+ \rightarrow \pi^+ \nu \bar{\nu}$  with high precision, provides such an opportunity. This is a compelling opportunity that should be exploited.
- Longer term, *Project X* at Fermilab can become the dominant facility in the world for rare kaon decay experiments. Its potential to provide ultra-high intensity kaon beams with tunable time structure is unprecedented. While the physics case for *Project X* is much broader than its capabilities for kaon experiments, the power of a *Project X* kaon program is a strong argument in its favor.
- Back-and-forth between theory and experiment has always led to unexpected progress in quark-flavor physics, and this is expected to continue. Therefore, stable support for theorists working in this area is essential. Lattice QCD plays a crucial role, and support for the computing facilities needed for LQCD progress should be maintained.

Quark flavor physics will be the source of future discoveries. A healthy U.S. particle physics program will endeavor to be among the leaders in this research.

## References

- [1] J. L. Hewett *et al.*, arXiv:1205.2671 [hep-ex].
- [2] M. Kobayashi and T. Maskawa, Prog. Theor. Phys. **49**, 652 (1973).
- [3] N. Cabibbo, Phys. Rev. Lett. **10**, 531 (1963).
- [4] S.L. Glashow, J. Iliopoulos, and L. Maiani, Phys. Rev. D **2**, 1285 (1970).
- [5] M.K. Gaillard and B.W. Lee, Phys. Rev. D **10**, 897 (1974).
- [6] A.I. Vainshtein and I.B. Khriplovich, Pisma Zh. Eksp. Theor. Fiz. **18**, 141 (1973) [JETP Lett. **18**, 83 (1973)].
- [7] G. Isidori, Y. Nir and G. Perez, Ann. Rev. Nucl. Part. Sci. **60**, 355 (2010) [arXiv:1002.0900 [hep-ph]]; and updates in G. Isidori, arXiv:1302.0661 [hep-ph].
- [8] A. Höcker, H. Lacker, S. Laplace and F. Le Diberder, Eur. Phys. J. C **21**, 225 (2001) [hep-ph/0104062]; and updates at <http://ckmfitter.in2p3.fr/>.
- [9] J. Charles *et al.*, Eur. Phys. J. C **41**, 1 (2005) [hep-ph/0406184].
- [10] L. Wolfenstein, Phys. Rev. Lett. **51**, 1945 (1983).
- [11] A. Hocker and Z. Ligeti, Ann. Rev. Nucl. Part. Sci. **56**, 501 (2006) [hep-ph/0605217].
- [12] Z. Ligeti, Int. J. Mod. Phys. A **20**, 5105 (2005) [hep-ph/0408267].
- [13] M. Bona *et al.* [UTfit Collaboration], JHEP **0803**, 049 (2008) [arXiv:0707.0636]; and updates at <http://utfit.org/>.
- [14] A. Lenz *et al.*, Phys. Rev. D **86** (2012) 033008 [arXiv:1203.0238 [hep-ph]].
- [15] Y. Grossman, Z. Ligeti and Y. Nir, Prog. Theor. Phys. **122**, 125 (2009) [arXiv:0904.4262 [hep-ph]].
- [16] J. Brod, contribution to “Kaon Physics with Project X”, in Ref. [17].
- [17] A. S. Kronfeld *et al.*, arXiv:1306.5009 [hep-ex].
- [18] S. Jäger, talk given at the NA62 Physics Handbook Workshop, <http://indico.cern.ch/get-File.py/access?contribId=5&resId=0&materialId=slides&confId=65927>
- [19] A. J. Buras, P. Gambino, M. Gorbahn, S. Jäger and L. Silvestrini, Nucl. Phys. B **592**, 55 (2001) [hep-ph/0007313].
- [20] M. Bauer, S. Casagrande, U. Haisch and M. Neubert, JHEP **1009**, 017 (2010) [arXiv:0912.1625 [hep-ph]].
- [21] M. Blanke, A. J. Buras, S. Recksiegel, C. Tarantino and S. Uhlig, JHEP **0706**, 082 (2007) [arXiv:0704.3329 [hep-ph]].
- [22] A. J. Buras and L. Silvestrini, Nucl. Phys. B **546**, 299 (1999) [hep-ph/9811471].
- [23] A. J. Buras, G. Colangelo, G. Isidori, A. Romanino and L. Silvestrini, Nucl. Phys. B **566**, 3 (2000) [hep-ph/9908371].
- [24] U. Haisch, contribution to “Kaon Physics with Project X”, in Ref. [17].
- [25] S. Adler *et al.* (E949 & E787 Collaborations), Phys. Rev. D **77**:052003 (2008) [arXiv:0709.1000]
- [26] Y. Grossman and Y. Nir, Phys. Lett. B **398**, 163 (1997) [hep-ph/9701313].
- [27] M. Blanke, Acta Phys. Polon. B **41**, 127 (2010), [arXiv:0904.2528]
- [28] F. Mescia, C. Smith and S. Trine, JHEP **0608**, 088 (2006) [hep-ph/0606081].

- [29] M. Blanke, A. J. Buras, B. Duling, K. Gemmler and S. Gori, *JHEP* **0903**, 108 (2009) [arXiv:0812.3803 [hep-ph]].
- [30] M. Blanke, A. J. Buras, B. Duling, S. Recksiegel, and C. Tarantino, *Acta Phys. Polon B* **41**, 657 (2010) [arXiv:0906.5454 [hep-ph]].
- [31] A. J. Buras, F. De Fazio and J. Girrbach, *JHEP* **1302**, 116 (2013) [arXiv:1211.1896 [hep-ph]].
- [32] A. J. Buras, T. Ewerth, S. Jäger and J. Rosiek, *Nucl. Phys. B* **714**, 103 (2005) [hep-ph/0408142].
- [33] J. F. Kamenik and C. Smith, *JHEP* **1203**, 090 (2012) [arXiv:1111.6402 [hep-ph]].
- [34] V. Cirigliano and I. Rosell, *Phys. Rev. Lett.* **99**, 231801 (2007) [arXiv:0707.3439 [hep-ph]].
- [35] V. P. Efrosinin, I. B. Khriplovich, G. G. Kirilin and Y. G. Kudenko, *Phys. Lett. B* **493**, 293 (2000) [hep-ph/0008199].
- [36] <http://na62.web.cern.ch/na62/Documents/ReferenceDocuments.html>.
- [37] <http://koto.kek.jp/>.
- [38] <http://trek.kek.jp/>.
- [39] <http://www.lnf.infn.it/kloe2/>.
- [40] J. Comfort *et al.*, FERMILAB-PROPOSAL-1021 (2011).
- [41] KOPIO Experiment Proposal (2005), <http://www.bnl.gov/rsvp/KOPIO.htm>.
- [42] Lattice QCD at the intensity frontier, T. Blum *et al.* [USQCD Collaboration], available at <http://www.usqcd.org/documents/13flavor.pdf>.
- [43] J. Zupan, arXiv:1101.0134 [hep-ph].
- [44] R. Aaij *et al.* [LHCb Collaboration], arXiv:1304.2600 [hep-ex].
- [45] R. Aaij *et al.* [LHCb Collaboration], *Phys. Rev. Lett.* **110** (2013) 021801 [arXiv:1211.2674 [hep-ex]].
- [46] A. J. Buras, J. Girrbach, D. Guadagnoli and G. Isidori, *Eur. Phys. J. C* **72** (2012) 2172 [arXiv:1208.0934 [hep-ph]].
- [47] K. De Bruyn *et al.*, *Phys. Rev. Lett.* **109**, 041801 (2012) [arXiv:1204.1737].
- [48] S. Chatrchyan *et al.* [CMS Collaboration], arXiv:1307.5025 [hep-ex], submitted to *Phys. Rev. Lett.*
- [49] R. Aaij *et al.* [LHCb Collaboration], arXiv:1307.5024 [hep-ex], submitted to *Phys. Rev. Lett.*
- [50] V. M. Abazov *et al.* [D0 Collaboration], *Phys. Rev. D* **84** (2011) 052007 [arXiv:1106.6308 [hep-ex]].
- [51] S. Laplace, Z. Ligeti, Y. Nir and G. Perez, *Phys. Rev. D* **65** (2002) 094040 [hep-ph/0202010].
- [52] Z. Xing *et al.* [LHCb Collaboration], arXiv:1212.1175 [hep-ex].
- [53] J. P. Lees *et al.* [BaBar Collaboration], arXiv:1303.0571 [hep-ex].
- [54] S. Fajfer, J. F. Kamenik, I. Nisandzic and J. Zupan, *Phys. Rev. Lett.* **109**, 161801 (2012) [arXiv:1206.1872 [hep-ph]].
- [55] G. T. Bodwin, E. Braaten, E. Eichten, S. L. Olsen, T. K. Pedlar and J. Russ, arXiv:1307.7425 [hep-ph].
- [56] T. Aushev *et al.* [Belle II Collaboration], arXiv:1002.5012 [hep-ex].
- [57] M. Bona *et al.* [SuperB Collaboration], [arXiv:0709.0451 [hep-ex]].
- [58] I. Adachi *et al.* [Belle Collaboration], *Phys. Rev. Lett.* **108** (2012) 171802 [arXiv:1201.4643 [hep-ex]].
- [59] B. Aubert *et al.* [BaBar Collaboration], *Phys. Rev. D* **79** (2009) 072009 [arXiv:0902.1708 [hep-ph]].
- [60] H. Ishino *et al.* [Belle Collaboration], *Phys. Rev. Lett.* **98** (2007) 211801 [arXiv:hep-ex/0608035].
- [61] J. P. Lees *et al.* [BaBar Collaboration], *Phys. Rev. D* **87** (2012) 052009 [arXiv:1206.3525 [hep-ph]].

- [62] J. Beringer *et al.* [Particle Data Group Collaboration], Phys. Rev. D **86**, 010001 (2012).
- [63] Y. Amhis *et al.* [Heavy Flavor Averaging Group], [arXiv:1207.1158 [hep-ex]], and updates at <http://www.slac.stanford.edu/xorg/hfag/>.
- [64] M. Gronau, Phys. Lett. B **627** (2005) 82 [arXiv:hep-ph/0508047].
- [65] M. Fujikawa *et al.* [Belle Collaboration], Phys. Rev. D **81** (2010) 011101 [arXiv:0809.4366 [hep-ex]].
- [66] J. Charles *et al.* [CKM Fitter Group], Phys. Rev. D **84** (2011) 033005 [arXiv:1106.4041 [hep-ph]].
- [67] B. Aubert *et al.* [BaBar Collaboration], Phys. Rev. D **81** (2010) 051101 [arXiv:0912.2453 [hep-ex]].
- [68] K. Hara *et al.* [Belle Collaboration], Phys. Rev. D **82** (2010) 071101 [arXiv:1006.4201 [hep-ex]].
- [69] J. P. Lees *et al.* [BaBar Collaboration], [arXiv:1207.0698 [hep-ex]].
- [70] I. Adachi *et al.* [Belle Collaboration], Phys. Rev. Lett. **110** (2013) 131801 [arXiv:1208.4678 [hep-ex]].
- [71] CDF  $B$ -physics results may be found at <http://www-cdf.fnal.gov/physics/new/bottom/bottom.html>.
- [72] DO  $B$ -physics results may be found at <http://www-d0.fnal.gov/Run2Physics/WWW/results/b.htm>.
- [73] A. A. Alves, Jr. *et al.* [LHCb Collaboration], JINST **3**, S08005 (2008).
- [74] R. Aaij *et al.*, JINST **8**, P04022 (2013) [arXiv:1211.3055 [hep-ex]].
- [75] R. Aaij *et al.* [LHCb Collaboration], LHCb-PUB-2012-006, Eur. Phys. J. C **73**, 2373 (2013) [arXiv:1208.3355 [hep-ex]]; See also a summary in LHCb-PUB-2012-009.
- [76] I. Bediaga *et al.* [LHCb Collaboration] CERN-LHCC-2012-007 ; LHCb-TDR-12.
- [77] S. Stone and L. Zhang, Phys. Rev. D **79**, 074024 (2009) [arXiv:0812.2832 [hep-ph]].
- [78] R. Aaij *et al.* [LHCb Collaboration], Phys. Rev. D **86**, 052006 (2012) [arXiv:1204.5643 [hep-ex]].
- [79] S. Chatrchyan *et al.* [CMS Collaboration], JHEP **1204**, 033 (2012) [arXiv:1203.3976 [hep-ex]].
- [80] G. Aad *et al.* [ATLAS Collaboration], Phys. Lett. B **713**, 387 (2012) [arXiv:1204.0735 [hep-ex]].
- [81] D. M. Straub, arXiv:1205.6094 [hep-ph].
- [82] R. Aaij *et al.* [LHCb Collaboration], arXiv:1304.6325 [hep-ex].
- [83] [CMS Collaboration], CMS-PAS-BPH-11-009, 2013.
- [84] [ATLAS Collaboration], ATLAS-CONF-2013-038, 2013.
- [85] R. Aaij *et al.* [LHCb Collaboration], Phys. Rev. Lett. **110**, **241802** (2013) [arXiv:1303.7125 [hep-ex]].
- [86] R. Aaij *et al.* [LHCb Collaboration], JHEP **1206**, 058 (2012) [arXiv:1204.1620 [hep-ex]].
- [87] R. Aaij *et al.* [LHCb Collaboration], JHEP **1206**, 141 (2012) [arXiv:1205.0975 [hep-ex]].
- [88] R. Aaij *et al.* [LHCb Collaboration], Phys. Rev. D **85**, 091103 (2012) [arXiv:1202.5087 [hep-ex]].
- [89] R. Aaij *et al.* [LHCb Collaboration], Phys. Rev. Lett. **110**, **222001** (2013) [arXiv:1302.6269 [hep-ex]].
- [90] R. Aaij *et al.* [LHCb Collaboration], Phys. Rev. D **85**, 112004 (2012) [arXiv:1201.5600 [hep-ex]].
- [91] R. Aaij *et al.* [LHCb Collaboration], Phys. Lett. B **724** (2013) [arXiv:1304.4518 [hep-ex]].
- [92] V. A. M. Heijne *et al.* [LHCb Collaboration], LHCb-CONF-2012-014, Frascati Phys. Ser. **56**, 162 (2012).
- [93] D. M. Asner, T. Barnes, J. M. Bian, I. I. Bigi, N. Brambilla, I. R. Boyko, V. Bytev and K. T. Chao *et al.*, Int. J. Mod. Phys. A **24**, S1 (2009) [arXiv:0809.1869 [hep-ex]].
- [94] M. Gersabeck *et al.* [LHCb Collaboration], arXiv:1209.5878 [hep-ex].
- [95] U. Wiedner, Prog. Part. Nucl. Phys. **66**, 477 (2011).
- [96] B. I. Eisenstein *et al.* [CLEO Collaboration], Phys. Rev. D **78**, 052003 (2008) [arXiv:0806.2112 [hep-ex]].

- [97] G. Rong, arXiv:1209.0085 [hep-ex].
- [98] A. Zupanc *et al.* [Belle Collaboration], arXiv:1212.3942 [hep-ex].
- [99] A. S. Kronfeld, arXiv:0912.0543 [hep-ph].
- [100] R. Aaij *et al.* [LHCb Collaboration], Phys. Rev. Lett. **110**, 101802 (2013) [arXiv:1211.1230 [hep-ex]].
- [101] A. F. Falk, Y. Grossman, Z. Ligeti and A. A. Petrov, Phys. Rev. D **65**, 054034 (2002) [hep-ph/0110317]; A. F. Falk, Y. Grossman, Z. Ligeti, Y. Nir and A. A. Petrov, Phys. Rev. D **69**, 114021 (2004) [hep-ph/0402204].
- [102] E. Golowich, J. Hewett, S. Pakvasa and A. A. Petrov, Phys. Rev. D **76**, 095009 (2007) [arXiv:0705.3650 [hep-ph]].
- [103] O. Gedalia, Y. Grossman, Y. Nir and G. Perez, Phys. Rev. D **80**, 055024 (2009) [arXiv:0906.1879 [hep-ph]]. M. Ciuchini *et al.*, Phys. Lett. B **655**, 162 (2007). [arXiv:hep-ph/0703204].
- [104] M. Artuso, B. Meadows and A. A. Petrov, Ann. Rev. Nucl. Part. Sci. **58**, 249 (2008); A. Ryd and A. A. Petrov, Rev. Mod. Phys. **84**, 65 (2012); S. Bianco, F. L. Fabbri, D. Benson and I. Bigi, Riv. Nuovo Cim. **26N7**, 1 (2003); [arXiv:hep-ex/0309021]. G. Burdman and I. Shipsey, Ann. Rev. Nucl. Part. Sci. **53**, 431 (2003); X. Q. Li, X. Liu and Z. T. Wei, Front. Phys. China **4**, 49 (2009).
- [105] I. I. Bigi, arXiv:0902.3048 [hep-ph].
- [106] R. Aaij *et al.* [LHCb Collaboration], Phys. Rev. Lett. **108**, 111602 (2012); T. Aaltonen *et al.* [CDF Collaboration], Phys. Rev. Lett. **109**, 111801 (2012); New measurements do not confirm those results: R. Aaij *et al.* [LHCb Collaboration], Phys. Lett. B **723**, 33 (2013);
- [107] M. Golden and B. Grinstein, Phys. Lett. B **222**, 501 (1989); J. Brod, A. L. Kagan and J. Zupan, Phys. Rev. D **86**, 014023 (2012); B. Bhattacharya, M. Gronau and J. L. Rosner, Phys. Rev. D **85**, 054014 (2012); I. I. Bigi and A. Paul, JHEP **1203**, 021 (2012); G. Isidori, J. F. Kamenik, Z. Ligeti and G. Perez, Phys. Lett. B **711**, 46 (2012); J. Brod, Y. Grossman, A. L. Kagan and J. Zupan, JHEP **1210**, 161 (2012); W. Altmannshofer, R. Primulando, C. -T. Yu and F. Yu, JHEP **1204**, 049 (2012); Y. Grossman, A. L. Kagan and J. Zupan, Phys. Rev. D **85**, 114036 (2012); H. -Y. Cheng and C. -W. Chiang, Phys. Rev. D **85**, 034036 (2012) [Erratum-ibid. D **85**, 079903 (2012)]; G. Hiller, Y. Hochberg and Y. Nir, Phys. Rev. D **85**, 116008 (2012); T. Feldmann, S. Nandi and A. Soni, JHEP **1206**, 007 (2012).
- [108] E. Golowich, J. Hewett, S. Pakvasa and A. A. Petrov, Phys. Rev. D **79**, 114030 (2009).
- [109] D. Atwood and A. Soni, Phys. Rev. D **68**, 033003 (2003) [hep-ph/0304085].
- [110] G. Pakhlova *et al.* [Belle Collaboration], Phys. Rev. Lett. **101**, 172001 (2008) [arXiv:0807.4458 [hep-ex]].
- [111] T. Blum *et al.* [USQCD Collaboration], *Lattice QCD at the Intensity Frontier*, <http://www.usqcd.org/documents/13flavor.pdf> (2013).
- [112] R. Brower *et al.* [USQCD Collaboration], *Fundamental parameters from future lattice calculations*, <http://www.usqcd.org/documents/fundamental.pdf> (2007).
- [113] J. Laiho, E. Lunghi and R. S. Van de Water, Phys. Rev. D **81**, 034503 (2010) [arXiv:0910.2928 [hep-ph]].
- [114] G. Colangelo *et al.* [FLAG], Eur. Phys. J. C **71**, 1695 (2011) [arXiv:1011.4408 [hep-lat]].
- [115] T. Blum *et al.* [RBC and UKQCD Collaborations], Phys. Rev. Lett. **108**, 141601 (2012) [arXiv:1111.1699 [hep-lat]].
- [116] T. Blum *et al.* [RBC and UKQCD Collaborations], Phys. Rev. D **86**, 074513 (2012) [arXiv:1206.5142 [hep-lat]].

- [117] P. A. Boyle *et al.* [RBC and UKQCD Collaborations], arXiv:1212.1474 [hep-lat].
- [118] N. H. Christ *et al.* [RBC and UKQCD Collaborations], Phys. Rev. Lett. **105**, 241601 (2010) [arXiv:1002.2999 [hep-lat]].
- [119] P. Junnarkar and A. Walker-Loud, arXiv:1301.1114 [hep-lat].
- [120] N. H. Christ, T. Izubuchi, C. T. Sachrajda, A. Soni and J. Yu [RBC and UKQCD Collaborations], arXiv:1212.5931 [hep-lat].
- [121] L. Lellouch and M. Luscher, Commun. Math. Phys. **219**, 31 (2001) [hep-lat/0003023].
- [122] T. Blum *et al.* [RBC and UKQCD Collaborations], Phys. Rev. D **84**, 114503 (2011) [arXiv:1106.2714 [hep-lat]].
- [123] C. Kelly *et al.* [RBC and UKQCD Collaborations], PoS LATTICE **2012**, 130 (2012).
- [124] J. Brod and M. Gorbahn, Phys. Rev. D **82**, 094026 (2010) [arXiv:1007.0684 [hep-ph]].
- [125] V. Cirigliano, G. Ecker, H. Neufeld, A. Pich and J. Portoles, Rev. Mod. Phys. **84**, 399 (2012) [arXiv:1107.6001 [hep-ph]].
- [126] M. T. Hansen and S. R. Sharpe, Phys. Rev. D **86**, 016007 (2012) [arXiv:1204.0826 [hep-lat]].
- [127] S. -W. Qiu *et al.* [Fermilab Lattice and MILC Collaborations], PoS LATTICE **2011** (2011) 289 [arXiv:1111.0677 [hep-lat]].
- [128] J. P. Lees *et al.* [BaBar Collaboration], Phys. Rev. Lett. **109**, 101802 (2012) [arXiv:1205.5442 [hep-ex]].
- [129] J. A. Bailey *et al.* [Fermilab Lattice and MILC Collaborations], Phys. Rev. Lett. **109**, 071802 (2012) [arXiv:1206.4992 [hep-ph]].
- [130] C. McNeile, C. T. H. Davies, E. Follana, K. Hornbostel and G. P. Lepage [HPQCD Collaboration], Phys. Rev. D **85**, 031503 (2012) [arXiv:1110.4510 [hep-lat]].
- [131] R. Zhou, arXiv:1301.0666 [hep-lat].
- [132] W. Detmold, C. -J. D. Lin, S. Meinel and M. Wingate, Phys. Rev. D **87**, 074502 (2013) [arXiv:1212.4827 [hep-lat]].
- [133] I. Baum, V. Lubicz, G. Martinelli, L. Orifici and S. Simula, Phys. Rev. D **84**, 074503 (2011) [arXiv:1108.1021 [hep-lat]].